EBioMedicine 11 (2016) 262–277

Contents lists available at ScienceDirect

EBioMedicine

journal homepage: www.ebiomedicine.com

Research Paper

Psychedelics Recruit Multiple Cellular Types and Produce Complex Transcriptional Responses Within the Brain

David A. Martin, Charles D. Nichols *

Department of Pharmacology and Experimental Therapeutics, Louisiana State University Health Sciences Center, New Orleans, LA 70112, USA

ARTICLE INFO

Article history:
Received 27 April 2016
Received in revised form 24 August 2016
Accepted 31 August 2016
Available online 3 September 2016

Keywords:
Neurons
Glia
Astrocytes
Psychedelics
Gene expression
mPFC
Serotonin
Immunofluorescence
FACS
Neurocytometry
5-HT2A

ABSTRACT

There has recently been a resurgence of interest in psychedelics, substances that profoundly alter perception and cognition and have recently demonstrated therapeutic efficacy to treat anxiety, depression, and addiction in the clinic. The receptor mechanisms that drive their molecular and behavioral effects involve activation of cortical serotonin 5-HT_{2A} receptors, but the responses of specific cellular populations remain unknown. Here, we provide evidence that a small subset of 5-HT_{2A}-expressing excitatory neurons is directly activated by psychedelics and subsequently recruits other select cell types including subpopulations of inhibitory somatostatin and parvalbumin GABAergic interneurons, as well as astrocytes, to produce distinct and regional responses. To gather data regarding the response of specific neuronal populations, we developed methodology for fluorescence-activated cell sorting (FACS) to segregate and enrich specific cellular subtypes in the brain. These methods allow for robust neuronal sorting based on cytoplasmic epitopes followed by downstream nucleic acid analysis, expanding the utility of FACS in neuroscience research.

1. Introduction

Classic serotonergic hallucinogens, also called psychedelics, produce profound cognitive and perceptual alterations in humans. Recently, there has been a resurgence of interest in the clinical study of psychedelics, and remarkable efficacy has been demonstrated in clinical trials for various psychiatric conditions such as anxiety (Gasser et al., 2014; Grob et al., 2011) and addiction (Bogenschutz et al., 2015; Johnson et al., 2014). A greater knowledge of the molecular mechanisms of action of psychedelics has the potential for further understanding of normal cognitive and perceptual behaviors, as well as several psychiatric disorders. Psychedelics are a class of drug that includes several distinct chemical structures. Although many psychedelics exhibit complex receptor pharmacology (Halberstadt and Geyer, 2011; Nichols, 2016), all are believed to exhibit their primary effects through activation of the brain serotonin 5-HT_{2A} receptor (Glennon et al., 1984; Halberstadt, 2015) in both humans (Vollenweider et al., 1998) and rodents (Gresch et al., 2007).

Serotonin 5-HT_{2A} receptor mRNA and protein are expressed in many brain regions, particularly the neocortex, but also in the claustrum, mammillary nucleus, amygdala, and striatum (Pasqualetti et al., 1996; Pazos et al., 1985; Weber and Andrade, 2010). Extensive work in rodents indicates that the cortex is a critical locus for their behavioral effects (Gonzalez-Maeso et al., 2007; Gresch et al., 2007). In humans, psychedelics can lead to increased [^{18}F]-fluorodeoxyglucose uptake (Vollenweider et al., 1997), decreased blood flow and blood oxygen level dependent (BOLD) signal (Carhart-Harris et al., 2012), and disruption of oscillations in several cortical regions (Riba et al., 2004; Muthukumaraswamy et al., 2013).

Activation of 5-HT_{2A} receptors in the cortex is necessary for the effects of psychedelics, but the role of individual cell types remains unknown. For example, systemic administration of psychedelics produces widespread gene expression changes in the prefrontal cortex (PFC) (Nichols et al., 2003; Nichols and Sanders-Bush, 2002) and somatosensory cortex (SSC) (Gonzalez-Maeso et al., 2003), but these data refer only to entire structures and not to their cellular constituents. Interestingly, a subset of deep pyramidal cells in layer V of the prefrontal cortex is directly depolarized by 5-HT_{2A} receptor activation in brain slices, implicating an intracortical mechanism in the action of psychedelics (Beique et al., 2007). It is also known that DOI causes GABA release and increases of cFos within Gad67-expressing cells in the PFC and orbital cortex (Abi-Saab et al., 1999; Wischhof and Koch, 2012), but the identity of the type of interneurons activated is unknown. Few studies have examined the activation of non-neuronal cells in the

* Corresponding author at: Department of Pharmacology and Experimental Therapeutics, LSU Health Sciences Center, 1901 Perdido St., New Orleans, LA, 70112, USA.
E-mail address: cnich1@lsuhsc.edu (C.D. Nichols).

http://dx.doi.org/10.1016/j.ebiom.2016.08.049

brain, although one report found an increase in cFos expression in oligodendrocytes of the PFC following LSD (Reissig et al., 2008). Understanding how individual cells within a particular cortical region respond to psychedelics and interact with each other will be crucial to understand fully their mechanism of action and for developing potential therapeutic applications.

Here, we demonstrate that psychedelics activate heterogeneous populations of cells in the medial PFC (mPFC) and SSC, including excitatory neurons, inhibitory neurons, and astrocytes. We show that immediate early gene induction within activated cells varies with brain region and cell type, and that a subset of 5-HT_{2A}-expressing neurons is activated by psychedelics and internalizes receptors following drug administration in several areas, including the mPFC, SSC, and claustrum. Our results support the hypothesis that a group of excitatory neurons is directly activated by psychedelics, and that other cell types, including somatostatin and parvalbumin interneurons, are subsequently recruited.

Significantly, to gather our data we developed methodology that allows robust sorting and purification of cells by FACS utilizing cytoplasmic and extracellular membrane epitopes. For example, these techniques allowed us to segregate and purify large populations of somatostatin and parvalbumin GABAergic interneurons using non-nuclear markers. The ability to sort and purify large cellular populations from whole brain tissues using non-nuclear markers significantly expands the utility of 'neurocytometry' – a term for the analysis of brain cells with flow cytometry. Overall, neurocytometry is more rapid and cost effective than existing methods of sorting whole brain cells such as single cell laser capture.

2. Methods

2.1. Animals, Drugs, and Treatment

Male Sprague-Dawley rats obtained from Harlan (Indianapolis, IN) were between 250 and 300 g upon arrival, and between 300 and 350 g during treatment. Animals were housed individually for at least seven days before treatment, during which time they were handled for 10 min each day. Rats were individually housed in translucent home cages, allowed free access to food and water, and kept on a 12:12 h light/dark cycle. Rats were injected (i.p.) with either sterile saline or (*R*)-DOI·HCl (6.0 mg/kg) during their dark cycle, and placed back into their home cage for 105 min. Following this interval, the rats were briefly anesthetized with isoflurane and decapitated. Rats were processed in pairs on each day of experimentation; one control and one drug-treated animal were always processed together in parallel. The entire brain was dissected within 3 min, and either frozen in 2-methyl butane cooled with dry ice for 20 s (prior to Method A), or cut into 2 mm coronal sections and immediately submerged into ice-cold, freshly prepared 4% paraformaldehyde in PBS (prior to Method B). Frozen brains were stored at −80 °C until further processing. (*R*)-DOI·HCl was synthesized in the laboratory of Dr. D.E. Nichols at Purdue University. Animals used in these studies were maintained in accordance with the U.S. Public Health Service Policy on Humane Care and Use of Laboratory Animals, and all protocols were approved by the Institutional Animal Care and Use Committees of LSUHSC.

2.2. Brain Dissection and Neuronal Dissociation (Method A)

These dissociation and FACS procedures were adapted, with modifications, from the Hope Laboratory at NIDA (Guez-Barber et al., 2012; Liu et al., 2014). Frozen brains were sliced into 1 mm thick coronal sections from +3.7 mm to +2.7 mm, +2.7 mm to +1.7 mm and +1.7 to +0.7 mm, relative to bregma. Razors were used to dissect the frozen mPFC from the two anterior slices and the SSC from the posterior slice. The tissue was kept chilled on ice for all of the remaining procedures. Frozen brain tissue was covered in several drops of Hibernate-A (Brain-Bits) neuronal media to thaw on a cold glass plate. The brain regions were minced in Hibernate-A with razors 200 times in orthogonal directions until a mushy consistency was achieved. The solution was then pipetted into a chilled microfuge tube (Protein LoBind 1.5 ml, Eppendorf), in which Hibernate-A was added to a total volume of 600 μl. The solution was allowed to settle for 5 min. The supernatant was transferred into another tube and an additional 500 μl of Hibernate A was added to the sample. This solution was pipetted back and forth 15 times through a fire-polished glass Pasteur pipette with a tip diameter of ~0.6 mm. After 5 min, the supernatant containing additional dissociated cells was combined with the initial supernatant. The dissociated cells (~1 ml) were filtered sequentially through pre-wetted 100 μm and 40 μm filters and stained.

2.3. Neuronal Soma Fixation and Dissociation (Method B)

Fresh, 2 mm coronal sections immersion fixed in cold 4% paraformaldehyde for 10–12 h were transferred to PBS and washed 4× for 10 min each. The mPFC (+3.7–+1.7 mm) and SSC (+1.7 to −0.7 mm) were then dissected, as above, and placed into a cold solution of PBS supplemented with 0.1% Tween-20 (PBS-T). The brain sections were then minced with sharp razors on an ice-cold glass plate for 5 min. The tissue was collected in PBS-T, and spun at 300 ×g for 5 min. The supernatant was removed, and tissue was resuspended in 1 ml Accutase enzymatic solution, and pushed back and forth 10× through a 1 ml syringe connected to a 19 G needle. The tissue was incubated while shaking at room temperature for 1 h. After removal of the enzyme and rinse with cold PBS-T, the tissue was passed back and forth 10 times through a syringe coupled to a 21 G needle. After settling for 5 min, the supernatant was removed and 500 μl of PBS-T was added to the tissue. The trituration cycle was completed sequentially with a 23 G needle and then twice more with a 25 G needle. Following each set of 10 triturations, the supernatant was collected after 5 min of settling. Trituration cycles were completed on ice. After all trituration cycles were completed, the supernatants were combined and filtered through a 70 μm mesh filter before staining.

2.4. FACS Antibody Staining

The filtrate was transferred into low protein-binding 1.5 ml microfuge tubes (Eppendorf) for antibody staining. Staining carried out on unfixed cells (Method A) was performed with primary antibodies pre-conjugated by the manufacturer to fluorescent secondary antibodies, including α-phospho-cFos-AlexaFluor647 (1:400, Cell Signaling; RRID: AB_11178518). This antibody is directed against a synthetic phosphopeptide corresponding to Ser32 of cFos. Phosphorylation of cFos at this residue has been shown to result in increased stability and nuclear localization of the protein (Sasaki et al., 2006). Other antibodies were: α-NeuN-Phycoerythrin (1:800, Millipore; RRID: AB_11212465); α-GFAP-AlexaFluor488 (1:500, BD Pharmingen; RRID: AB_1645350). Cells were simultaneously incubated with 4′,6-diamidino-2-phenylindole (DAPI) to stain nuclei at a final concentration of 1.43 μM. Incubations were performed on a rotator at 4 °C for 90 min in Hibernate A.

Staining of fixed neurons using Method B utilized the following primary antibodies: goat-α-somatostatin (1:200, Santa Cruz; RRID: AB_2302603); rabbit-α-parvalbumin PV-25 (1:15,000, Swant; RRID: AB_10000344); and mouse-α-cFos C-10 (1:300, Santa Cruz; RRID: AB_10610067). Primary incubations were performed for 1.5 h shaking at RT in PBS with 0.1% Tween-20, supplemented with 1000 U/ml RNase inhibitor (RNAsin, Promega) and 1 mm dithiothreitol (DTT). Two washes in cold PBS-T were followed by secondary incubations with the appropriate secondaries at 4 °C in PBS-T. All secondaries were highly cross adsorbed and used at a concentration of (1:750): α-goat-647 (Jackson; RRID: AB_2340437), α-mouse-488 (Jackson; RRID: AB_2338854), α-rabbit-647 (Invitrogen; RRID: AB_2535813). DAPI (1.43 μm) was also included in secondary incubations. Following secondary incubations,

cells were washed two times and resuspended in 500 μl of PBS-T, containing α-NeuN-Phycoerythrin (1:800, Millipore) for FACS. Stained cells were transferred to 5 ml tubes for flow cytometry and kept on ice until cell sorting.

2.5. FACS

All samples were sorted on a BD FacsAria into empty 1.7 ml microfuge tubes. The sample loader and collection tubes on the cell

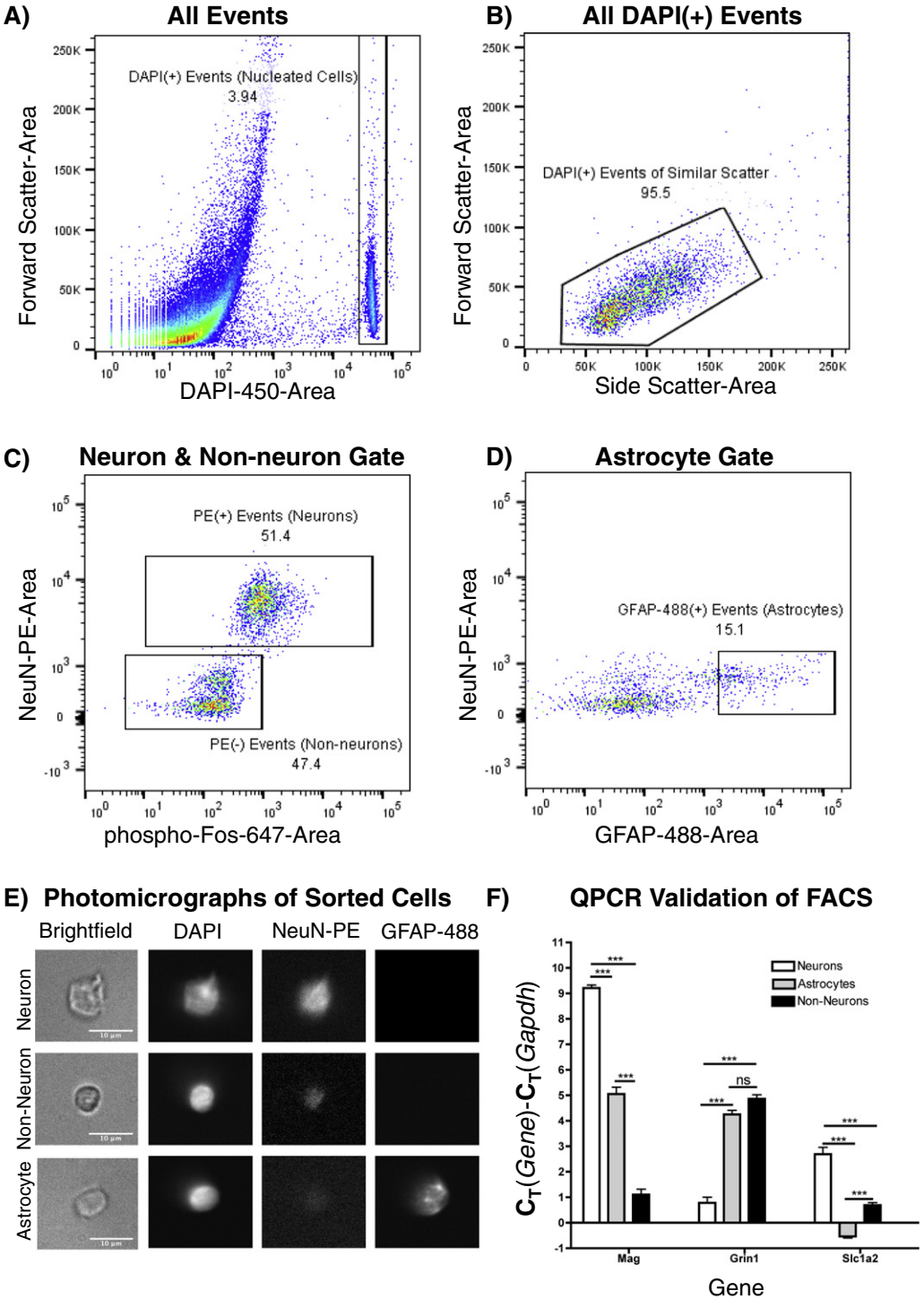

Fig. 1. FACS gating strategy: Data are from a representative sort of mPFC; all runs produced similar patterns. Numbers represent percentages of cells within gates. A) All events are shown. DAPI(+) gate includes cells and excludes debris. B) Forward and Side Scatter gates eliminate irregularly-shaped DAPI(+) events. C) NeuN-PE(+) events represent neurons, whereas Neun-PE(−) events represent non-neurons. D) NeuN-PE(−)/GFAP-488(+) events represent astrocytes. E) Appearance of representative sorted cells (63×) in brightfield (left), DAPI (left middle), PE (right middle), and 488 (right) channels. Sorted neurons (top), non-neurons (middle), and astroctyes (bottom). G) Expression levels of cell-type-enriched mRNA markers in sorted cells, relative to *gapdh* expression. "***" & "ns" indicate $p < 0.001$ & non-significant. One-way ANOVA, Tukey post-hoc performed between all groups ($N = 6$, astrocytes and non-neurons; $N = 12$, neurons).

sorter were kept at 4 °C. Compensation for spectral overlap between phycoerythrin (PE) and AlexaFluor-488 fluorophores was applied based on the analysis of singly stained samples. 100,000 events from each sample were analyzed to set gates prior to cell sorting. The gating strategy for cell sorting following Method A is shown in Fig. 1. A population of cell bodies, defined as the events falling within a narrow band of high DAPI fluorescence and displaying clustered forward- and side-scatter characteristics, comprised 4.4% (range 2.9–5.5%) of the total events on average for each run; the remaining 95.6% (range 94.5–97.1%) of events was comprised of cellular debris and was excluded from further gating. A clear segregation between neuronal and non-neuronal populations was apparent based on NeuN-PE immunoreactivity (IR) and these populations were verified by downstream QPCR analysis (Fig. 1). A continuum of phospho-cFos-647 fluorescence intensity was observed within the PE(+) (neuronal) population, and the PE(+) population was subdivided such that "Fos(+)" populations consist of PE(+) neuronal events that were in the top ~2.5% of phospho-cFos-647 emission intensity, and "Fos(−)" populations consist of the lowest ~80% of PE(+) neurons with respect to phospho-cFos-647 emission intensity. During the course of each run, 2 non-neuronal populations were sorted, sequentially: 1) Non-neurons as all PE(−) events 2) Astrocytes as PE(−)/GFAP-488(+) events. GFAP-488(+) events were defined as events in the top 15% of GFAP-488-emission intensity within the PE(−) (Non-neuronal) group. Therefore, 4 populations were sorted: 1) Fos(+) neurons; 2) Fos(−) Neurons; 3) All Non-neurons; 4) GFAP(+) Non-neurons. An aliquot of dissociated, but unsorted, cells/debris from each sample was also frozen at −80 °C for QPCR analysis of unsorted tissue.

The sorting strategy following Method B is illustrated in Figs. 8–9. A population of neuronal somata, consisting of 11.3% (range 9.5–13.5%) of total events, was found to display a single, narrow peak of DAPI fluorescence. Neurons were defined as NeuN-PE(+) events, the threshold being set by manual inspection and varying little between individual runs. These cells were further gated to exclude events with high side scatter-height, which were found in preliminary experiments to emit high levels of background fluorescence and compromise sorted-cell purity. Individual neuronal subtypes, somatostatin(+) and parvalbumin(+), were sorted in separate runs. Subtype-specific gates were defined to compensate for the increase in 647-height which correlates with side scatter-area, as seen in Figs. 8–9. The shape of these gates was drawn to include events which clearly lie above the background level of fluorescence, apparent from the inspection of the 647-height intensity of DAPI(−) events. Somatostatin(−) and parvalbumin(−) events were gated to include NeuN(+) events that were within background levels of light intensity with respect to 647-height and side-scatter area (~80%), to exclude highly and moderately labeled somatostatin and parvalbumin neurons. Within each subtype, cFos(+) and cFos(−) populations were also gated. cFos(+) gates were set to include the highest 5% c-Fos-488-height events for subtype(−) cells, and highest 10% for subtype(+) cells. cFos(−) gates were set to include the bottom 75% cFos-488-height events for both subtype(+) and subtype(−) cells. It may be noted that cFos-488-height levels do not vary significantly with scatter, as this is a nuclear stain and nuclei size is relatively constant in neurons.

2.6. RNA Extraction

Tubes containing sorted cell populations were centrifuged at 13,000 g and the supernatant was removed before freezing at −80 °C until RNA extraction. RNA extraction was performed with Trizol, according to manufacturer's directions with modifications. Following Method A, cells were vortexed with 100 μl Of Trizol, phase separated with 5 μl of bromo-anisole, and spun at 13,000 g for 15 min. The supernatant was added to 50 μl of isopropanol with 1 μg of glycogen to aid in pellet formation, spun 13,000 g for 6 min, and washed with 75% ethanol. Pellets were resuspended in 10 μl nuclease-free water. Following Method B, cells were incubated overnight in 70 μl of RNA extraction buffer at 60 °C for 16 h. RNA extraction buffer consists of 15 mM Tris–HCL, pH = 8.0, 1% SDS, and 4 mg/ml Proteinase K. This solution was then extracted with 150 μl TRIzol as above, with all other reactants scaled up accordingly.

2.7. RTQPCR

First strand cDNA was synthesized using the ImPromp-II kit from Promega (Madison, WI) using all RNA extracted from each sample. For the quantitative RT-PCR (QPCR) experiments, the Universal ProbeLibrary system from Roche (Indianapolis, IN) was used to design primer/probe pairs. Primers were synthesized by IDT (Coralville, IA). Primer sequences can be found in Supplementary Fig. S3. Duplicate amplification reactions were performed on a Roche 480 LightCycler II using the Roche Light Cycler Master Mix following the manufacturer's directions. Amplification of *gapdh*, a housekeeping gene, was performed simultaneously in every well to normalize amplification thresholds to input cDNA quantity. Relative expression for each gene of interest (GOI) was determined by subtracting the *gapdh* amplification threshold from the GOI threshold for each sample well, using the point of 2nd derivative maximum, as estimated by the Roche software package. It should be noted when interpreting data that different sorted groups of cells may have varied levels of *gapdh*/total mRNA as these cells are not composed of the same cell-types. Statistical analyses of QPCR relative expression data (# of cycles from *gapdh* amplification) were performed using a one-way analysis of variance (ANOVA) between compared groups for each GOI. Tukey's multiple comparisons testing was used to compare every possible pair of samples, and significance levels were set at $p < 0.05$. Bar graphs always display mean ± SEM.

2.8. Immunofluorescence

Flash frozen brains were stored at −80 °C until processing. Coronal sections (30 μm) were sliced on a cryostat and thaw mounted onto permafrost slides. These slices were immediately dipped into fresh 4% paraformaldehyde in PBS for somatostatin and cFos staining, or 95% ethanol for 5-HT_{2A}, cFos, and Gad67 staining. The sections were fixed for 45 min at room temperature and washed 3× in PBS before blocking for 30 min in PBS with 2.5% donkey serum and 0.25% Triton. Sections were stained on the slides for 2.5 h at room temperature, shaking in primary antibody solution diluted in blocking buffer. The following antibodies were used: rabbit-α-cFos 9F6 (1:300, Cell Signaling; RRID: AB_2247211), goat-α-somatostatin D-20 (1:200, Santa Cruz; RRID: AB_2302603), mouse-α-cFos C10 (1:200, Santa Cruz; RRID: AB_10610067), rabbit-α-5-HT_{2A} (1:150, Neuromics; RRID: AB_1612272), mouse-α-Gad67 MAB5406 (1:1000, Millipore; RRID: AB_2278725). Following primary incubation, slides were washed 3× in PBS before incubating in the appropriate secondaries (1:500) for 1.5 h at room temperature. Slides were then washed twice in PBS and coverslipped in mounting medium (Cytoseal 280). All antibodies that we used for FACS were also those we used in subsequent immunofluorescence experiments with brain slices (α-cFos, α-phospho-cFos, α-somatostatin, α-parvalbumin, α-GFAP, α-NeuN, α-5-HT2A, and α–Gad67). In every case for each antibody, (+) cell populations sorted utilizing a particular antibody demonstrated high expression of the mRNA for the gene encoding the protein target of the antibody, with (−) sorted populations having little to no mRNA expression for the same gene. Although gene expression levels often correlate with protein expression levels, this is not always the case. Therefore, some caution is warranted when interpreting this data with regard antibody selectivity.

Slides used for quantitative analysis were viewed and imaged on a Leica DMRA2 upright epifluorescence microscope. Control and drug-treated brains were processed together. Quantified images were acquired with identical exposure settings, and displayed with identical contrast/brightness settings. Quantification of co-labeling was

performed by two separate experimenters that were blinded to treatment condition and their counts were averaged. Other images for publication were acquired using a Zeiss epifluorescence microscope with an Olympus DP-72 wide field camera.

3. Results

3.1. Standard FACS Analysis of Cortical Cells

First, we slightly modified existing neurocytometric methodology (Guez-Barber et al., 2012) to separate neurons from non-neurons, activated neurons from non-activated neurons, and astrocytes from other non-neurons in the mPFC and SSC. Our gating strategy for a representative sort and the appearance of sorted cells is shown in Fig. 1A–E. RT-qPCR analysis validated the identity of cellular populations (Fig. 1F). As expected, high levels of neuronal transcripts (*grin1*) relative to glial transcripts (*mag, slc1a2*) were detected in neuronal compared to non-neuronal populations. Higher levels of astrocyte-specific transcripts (*slc1a2*), relative to oligodendrocyte transcripts (*mag*) were measured in astrocyte compared to general non-neuronal populations (Fig. 1F).

In general, cortical neurons exhibit a continuum of phospho-cFos (Ser32) expression (Fig. 2A). The psychedelic phenethylamine (*R*)-DOI (6.0 mg/kg, i.p.) induces phospho-cFos expression only in a small subset of cells, visible as an increase in the number of neurons exhibiting high levels of phospho-cFos IR in (*R*)-DOI treated rats compared to control rats (Fig. 2C). This differential distribution was present in all comparisons (N = 5/region) of (*R*)-DOI treated and control neurons. For both control and (*R*)-DOI groups "Fos(+)" neurons were gated as the highest 2.5% of phospho-cFos IR neurons and "Fos(−)" neurons as the lowest 80% of phospho-cFos IR neurons (Fig. 2A).

3.2. IEG Expression in Psychedelic-Activated Neurons

IEG expression is significantly higher in DOI-Fos(+) neurons than DOI-Fos(−) neurons for each IEG and brain region tested (Fig. 2B, D). Control brains also contained activated neurons with higher levels of IEGs in Con-Fos(+) compared to Con-Fos(−) groups for each brain region and IEG tested (Fig. 2B, D). DOI-Fos(+) cells had higher levels of *cfos*, *fosb*, and *egr2* expression compared to Con-Fos(+) cells in SSC. In mPFC, however, only *fosb* expression was significantly higher in DOI-Fos(+) than Control-Fos(+) cells (Fig. 2A, B). DOI-Fos(−) neurons generally exhibited similar levels of IEG expression relative to Control-Fos(−). Interestingly, *egr2* expression was increased between DOI-Fos(−) neurons relative to Con-Fos(−) neurons in the mPFC (Fig. 2B, D). Two IEGs (*cfos*, *fosb*) were measured in unsorted, dissociated brain tissue, and significant increases were found in the treated group, as expected (Fig. S1). Together, these data indicate that the expression of IEGs induced by (*R*)-DOI when measured in unsorted brain tissue is mostly due to transcriptional activation of a small subset of neurons. However, another subset of neurons in the mPFC appears to express *egr2,* but not high levels of phospho-cFos, in response to (*R*)-DOI.

3.3. Activated Neurons Express Higher Levels of htr2a mRNA

Analysis of the DOI-Fos(+) activated population of neurons revealed that they have significantly higher mRNA expression of 5-HT_{2A} receptor

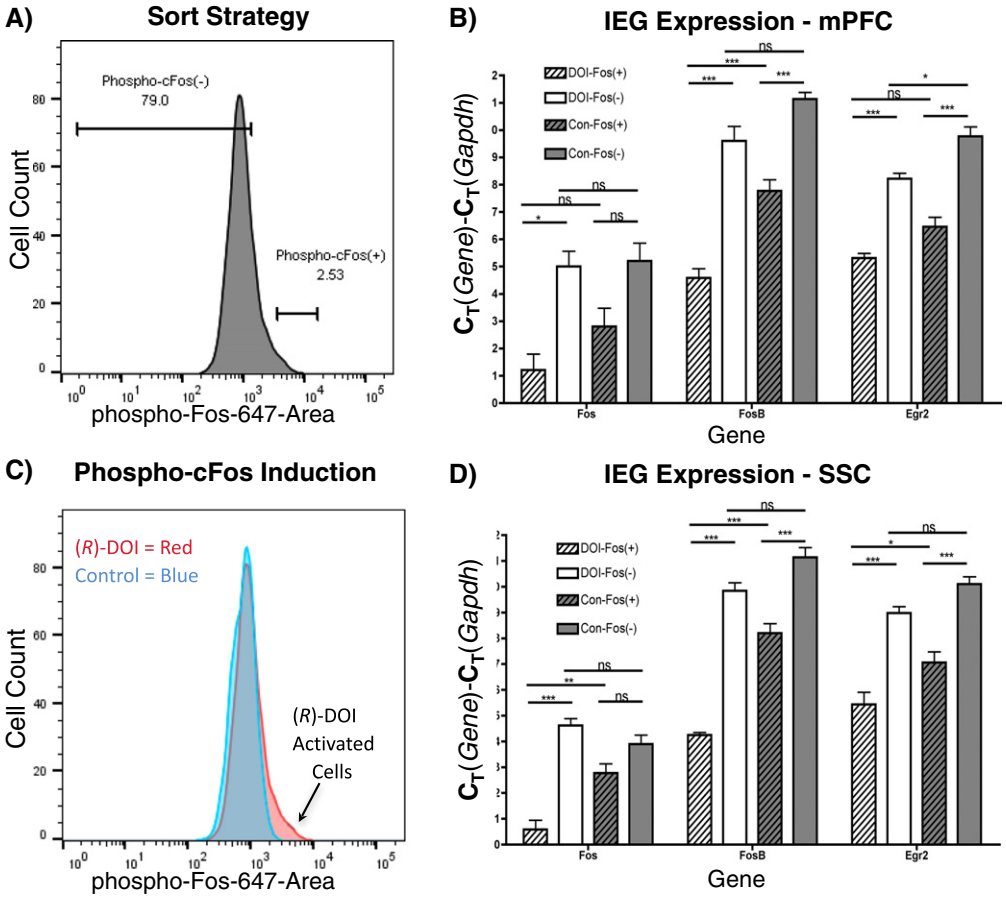

Fig. 2. Gating and IEG expression of Fos(+) and Fos(−) neurons: A) Representative FACS strategy for control and (*R*)-DOI treated neurons shown. Numbers represent percentages of cells within gates. B) Histogram overlay of mPFC neurons from (*R*)-DOI (red) and control (blue) animals with respect to phospho-cFos IR. C) IEG expression in sorted cells from mPFC. D) IEG expression from SSC. "*", "***", "****", and "ns" indicate $p < 0.05$, $p < 0.01$, $p < 0.001$, and non-significant, respectively. One-way ANOVA, Tukey post-hoc performed between all groups (N = 4–5/group). Only selected comparisons are shown.

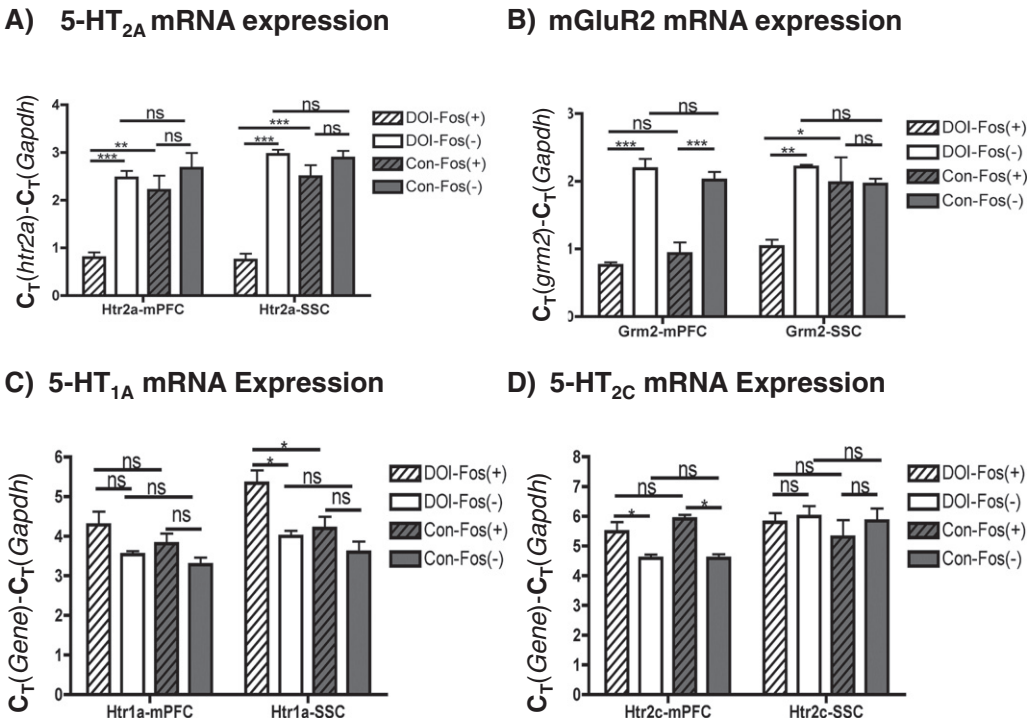

Fig. 3. GPCR gene expression in mPFC and SSC: A) *htr2a* levels in sorted cells. B) *grm2* levels in sorted cells. C) *htr2c* levels in sorted cells D) *htr1a* levels in sorted cells. "*", "**", "***", and "ns" indicate $p < 0.05$, $p < 0.01$, $p < 0.001$, and non-significant, respectively. One-way ANOVA, Tukey post-hoc performed between all groups (N = 4–5/group). Only selected comparisons are shown.

mRNA in both mPFC and SSC than non-activated neurons in these regions, implying a direct action of (*R*)-DOI on these neurons to activate IEG expression (Fig. 3A). By contrast, no enrichment of *htr2A* transcripts was found in Control-Fos(+) neurons relative to Control-Fos(−) neurons. To rule out the possibility that (*R*)-DOI may cause an increase in *htr2A* expression in Fos(+) cells, the levels of *htr2A* mRNA were measured in unsorted tissue and no difference between treated and untreated samples was found (Fig. S1). Therefore, drug-activated neurons contain higher levels of *htr2A* mRNA prior to drug administration. The metabotropic glutamate receptor 2 (mGluR2; *grm2*) has been previously demonstrated to functionally interact with the 5-HT_{2A} receptor (Benneyworth et al., 2007; Gewirtz and Marek, 2000; Marek et al., 2000). We found that *grm2* mRNA is more abundant in DOI-Fos(+) neurons compared to DOI-Fos(−) neurons in both the SSC and mPFC. However, this pattern was also true of Control-Fos(+) and Control-Fos(−) neurons in the mPFC (Fig. 3B). Therefore, DOI-Fos(+) neurons that respond to DOI are enriched in *grm2* transcripts relative to Control-Fos(+) neurons only in the SSC.

5-HT_{2C} receptor mRNA expression is not higher in (*R*)-DOI-activated neurons, even though (*R*)-DOI has high affinity for this receptor (Fig. 3C). We also found a significant decrease in 5-HT_{1A} receptor mRNA levels in DOI-Fos(+) neurons relative to DOI-Fos(−) neurons and to Control-Fos(+) neurons in the SSC, but not mPFC (Fig. 3D).

3.4. GABAergic Interneurons are Enriched in Activated Neurons

Because the neuronal population is comprised of both excitatory and inhibitory neurons, we examined for enrichment of GABAergic inhibitory neurons in the (*R*)-DOI activated population. In Control-Fos(+) neurons of the mPFC and SSC, very few transcripts specific for interneurons (*gad67*, *slc6a1*) were present relative to Control-Fos(−) neurons, indicating that few interneurons produce phospho-cFos under baseline conditions (Fig. 4A, B). DOI-Fos(+) neurons of the mPFC and SSC, however, contained levels of *gad67* and *slc6a1* that were comparable to DOI-Fos(−) neurons, and much higher than Control-Fos(+) neurons (Fig. 4A, B). To rule out the possibility that some neurons produced more cell-type specific transcripts in response to (*R*)-DOI, *gad67* levels were measured in unsorted tissue and no difference was detected between treated and control conditions (Fig. S1). These data indicate that GABAergic interneurons are activated by (*R*)-DOI, consistent with previous reports (Abi-Saab et al., 1999; Wischhof and Koch, 2012). Also, levels of the excitatory cell marker *slc17a7* (Vglut1) were measured and no significant difference in expression levels between any group was found. Interestingly, DOI-Fos(+) neurons contained more *slc17a6* (Vglut2) mRNA than DOI-Fos(−) neurons in the SSC, a pattern absent in controls (Fig. 4B). Therefore, a subset of cells in SSC that express VGlut2 is likely preferentially activated by (*R*)-DOI.

To determine which of the many subtypes of GABAergic cells are recruited by (*R*)-DOI, we examined levels of several interneuron-subtype-specific genes (*sst*, *pvlb*, *calb2*, *htr3a*) in sorted cell populations. These markers are produced in largely mutually exclusive interneuron subtypes, that together account for nearly all inhibitory neurons (Kubota and Kawaguchi, 1994; Rudy et al., 2011). We either failed to detect or detected only exceedingly low amounts of *calb2* and *htra3* mRNA in Fos(+) samples from both the treated and control groups (not shown), indicating that calretenin and 5-HT_3 expressing GABAergic cells are not the interneurons recruited by (*R*)-DOI. However, we found a large and significant increase in *pvlb* mRNA in DOI-Fos(+) compared to Con-Fos(+) neurons in both mPFC and SSC (Fig. 4A, B), and an increase in *sst* mRNA in DOI-Fos(+) neurons relative to Con-Fos(+) neurons only in SSC (Fig. 4B). No changes in *sst* mRNA were detected in unsorted tissues (Fig. S1), indicating that (*R*)-DOI does not alter levels of this gene. These data suggest that subsets of parvalbumin and somatostatin interneurons respond to (*R*)-DOI, but that the response differs by brain region.

3.5. Psychedelics Activate Non-neuronal Cells

The sorted non-neuronal populations from the SSC and mPFC (Fig. 1) are comprised of multiple cell types. As a heterogeneous group, we

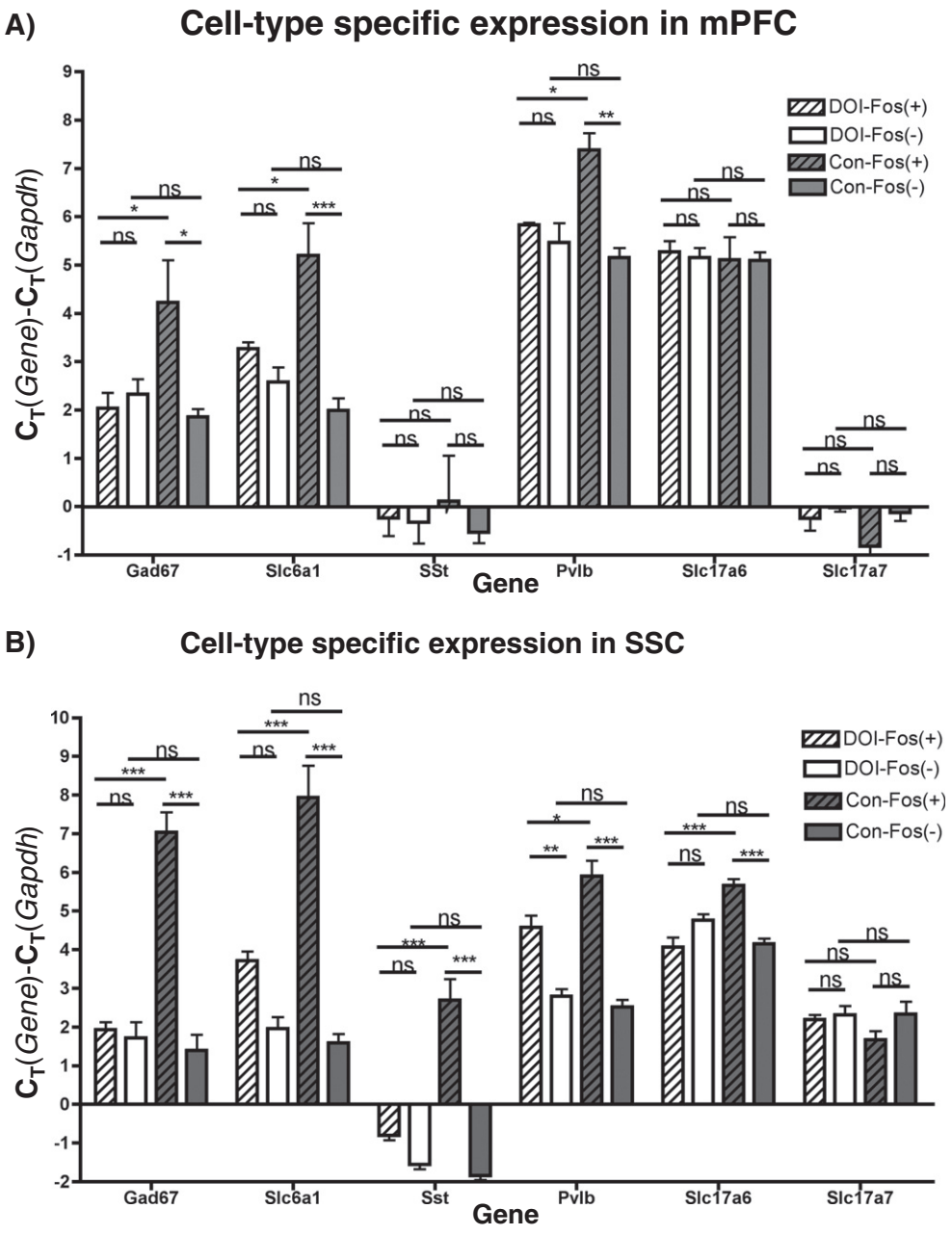

Fig. 4. Cell-type marker gene expression in mPFC and SSC: Levels of cell-type specific marker genes in mPFC (A) and SSC (B) in sorted cells. "*", "***", "****", and "ns" indicate $p < 0.05$, $p < 0.01$, $p < 0.001$, and non-significant, respectively. One-way ANOVA, Tukey post-hoc performed between all groups (N = 4–5/group). Only selected comparisons are shown.

measured an increase in *cfos* levels in drug-treated non-neurons vs. control non-neurons (Fig. S2). This result led us to hypothesize that (*R*)-DOI also affects glia and astrocytes. Astrocyte populations were sorted from other non-neurons by using an antibody directed against GFAP, an astrocyte marker. Astrocytes were found to be transcriptionally activated by (*R*)-DOI, and in treated samples of both SSC and mPFC, astrocytes had higher expression levels of *cfos* (Fig. S2). DOI-activated astrocytes also had higher levels of *per1* relative to Control-astrocytes in the mPFC and SSC (Fig. S2).

3.6. Immunohistochemistry Validation of Gene Expression and FACS Results

We performed immunohistochemistry and immunofluorescence experiments to validate our FACS and gene expression analyses results, and to locate cell-type specific activated cells in the cortex. In (*R*)-DOI-treated animals, we observed cFos-immunoreactivity (IR) increases that were clearly localized to a densely stained band in layer Va immediately below granular layer IV in the SSC, a wider, moderately stained area in deep layer V, and a distinct thin layer along the subplate, just superficial to the white matter (Fig. S3), consistent with previous reports (Leslie et al., 1993; Mackowiak et al., 1999; Scruggs et al., 2000; Tilakaratne and Friedman, 1996). We also observed cFos(+) neurons in high density throughout the deep mPFC, claustrum, insular, and endopiriform cortex, and scattered in superficial layers I-III throughout the mPFC and SSC (Fig. S4B).

To confirm that somatostatin-containing neurons are activated by (*R*)-DOI, co-staining for cFos and somatostatin (SOM) was performed. Double labeled cells were scattered throughout the cortex from the medial to lateral areas, and in layers II-VI. This co-expression was quantified in the agranular motor cortex and in the primary SSC from the pial surface to the white matter (Fig. 5). Whereas very few SOM(+) neurons produce appreciable cFos-IR under control conditions in the

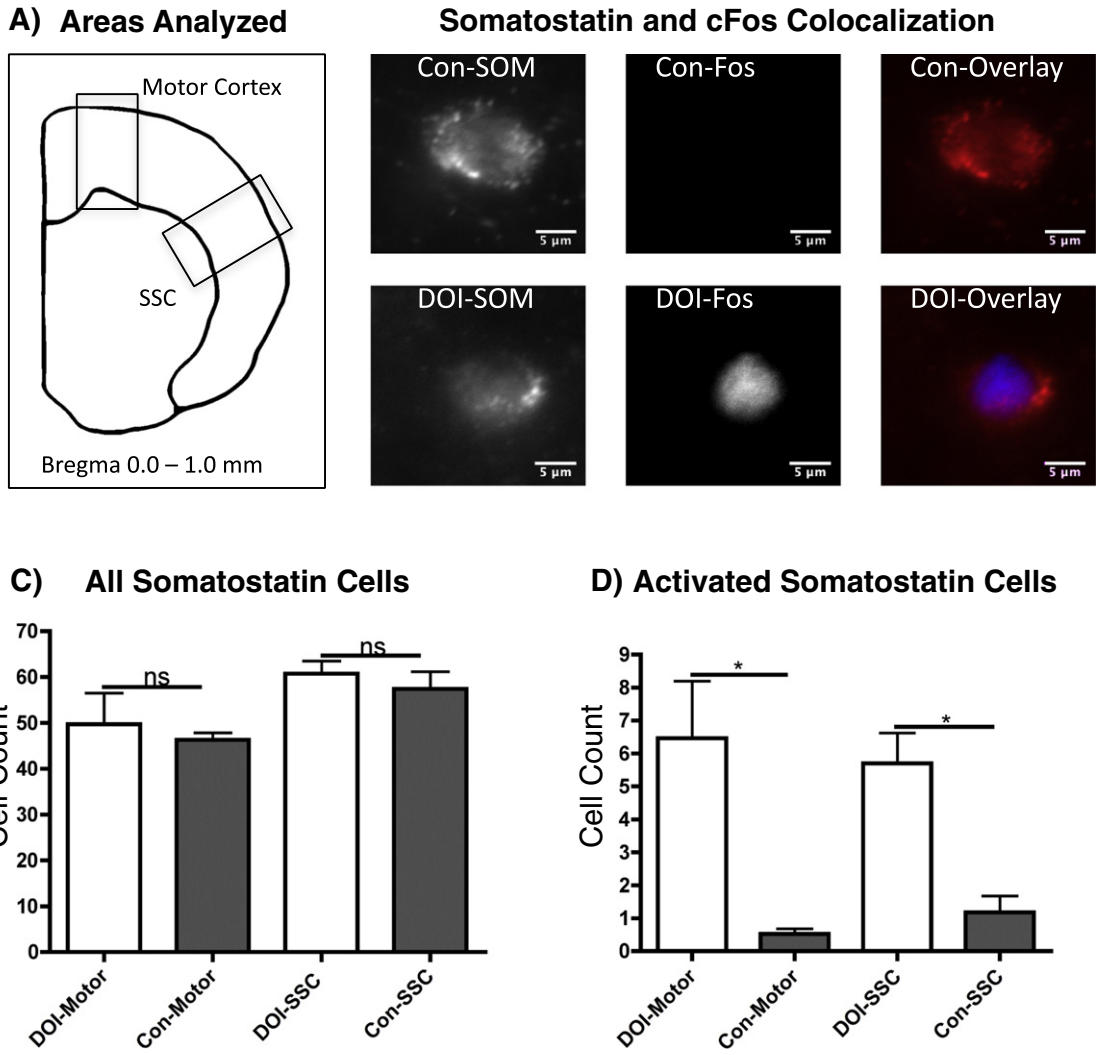

Fig. 5. Somatostatin and cFos quantification: Co-labeling for cFos and somatostatin in two brain regions was measured. A) Illustration indicating regions of quantification in motor cortex and SSC. B) Representative images (63×) of SOM(+) cells from control (top), and (*R*)-DOI (bottom) sections. C) Average counts of SOM(+) cells/region are shown. D.) Average counts of double-labeled SOM(+)/cFos(+) cells are shown. "*" and "ns" represent $p < 0.05$ and non-significant. Student's *t*-test, N = 3 animals/group; counts from at least 3 slices/animal were averaged per N.

motor and somatosensory areas (0.5% and 1.2%, respectively), (*R*)-DOI administration produces a robust induction of cFos-IR in SOM(+) cells of the motor cortex and SSC (13.0% and 9.4%, respectively) (Fig. 5). These results support the FACS data, and show that (*R*)-DOI activated SOM(+) interneurons are scattered throughout the parietal cortex.

3.7. (R)-DOI Produces 5-HT$_{2A}$ Receptor Internalization

We used a specific and well characterized rabbit polyclonal 5-HT$_{2A}$ antibody (Magalhaes et al., 2010; Weber and Andrade, 2010) to determine if there was a small population of cFos positive neurons that also expressed 5-HT$_{2A}$ receptor protein. In control animals, 5-HT$_{2A}$ IR displays a characteristic, diffuse banding pattern seen in previous studies with mice (Weber and Andrade, 2010), indicating expression is primarily on neuronal processes rather than soma (Fig. 6A, C, E). As such, cFos localization to 5-HT$_{2A}$ neurons was difficult to ascertain in cortex from control animals, as has been noted previously in mice (Weber and Andrade, 2010). Nevertheless, strong immunoreactivity within a band across layer V throughout frontal and parietal areas, and moderate immunoreactivity in layers I-III, deep layer V, and along the subplate was observed in controls.

Interestingly, 5-HT$_{2A}$ IR following (*R*)-DOI administration exhibited a very different pattern, clearly staining the peri-nuclear region and proximal processes of many cells throughout the cortex. These 5-HT$_{2A}$ receptor expressing cells were located in the areas of non-localizable staining present in the control brains (Fig. 6B, D, F), especially in deep layer V and along the cortical subplate (Fig. S4). Additional 5-HT$_{2A}$-labeled soma were located in layer Va, where 5-HT$_{2A}$ IR is most apparent in controls, although much staining in this region remains diffuse following (*R*)-DOI administration (Fig. S4). Superficial layer I-III neurons were also labeled in some areas of the motor and somatosensory cortices (Fig. 7, Fig. S5). We also observed that many neurons in lateral regions of the brain, including the orbital cortex, insula, endopiriform cortex, and claustrum, exhibited dramatic receptor redistribution, wherein neuronal somata and proximal processes can be clearly distinguished as containing 5-HT$_{2A}$ IR in treated animals, but not controls (Fig. 6). The majority of clearly labeled 5-HT$_{2A}$-containing cells did not express high levels of Gad67-IR (Fig. 6F), although a small subset of cells, primarily in layer V of the motor cortex and SSC, as well as in the endopiriform cortex, was found to co-express both proteins.

This (*R*)-DOI induced 5-HT$_{2A}$ receptor internalization allows for analysis of colocalization of cFos and 5-HT$_{2A}$ IR in treated animals. Indeed, cFos was induced in a small fraction of 5-HT$_{2A}$ neurons in each of the regions where 5-HT$_{2A}$ IR was observed, consistent with our FACS data. Colocalization was most extensive along the subplate, in deep layer V, in layer Va, and in the claustrum (Fig. S4). Frontal cortical

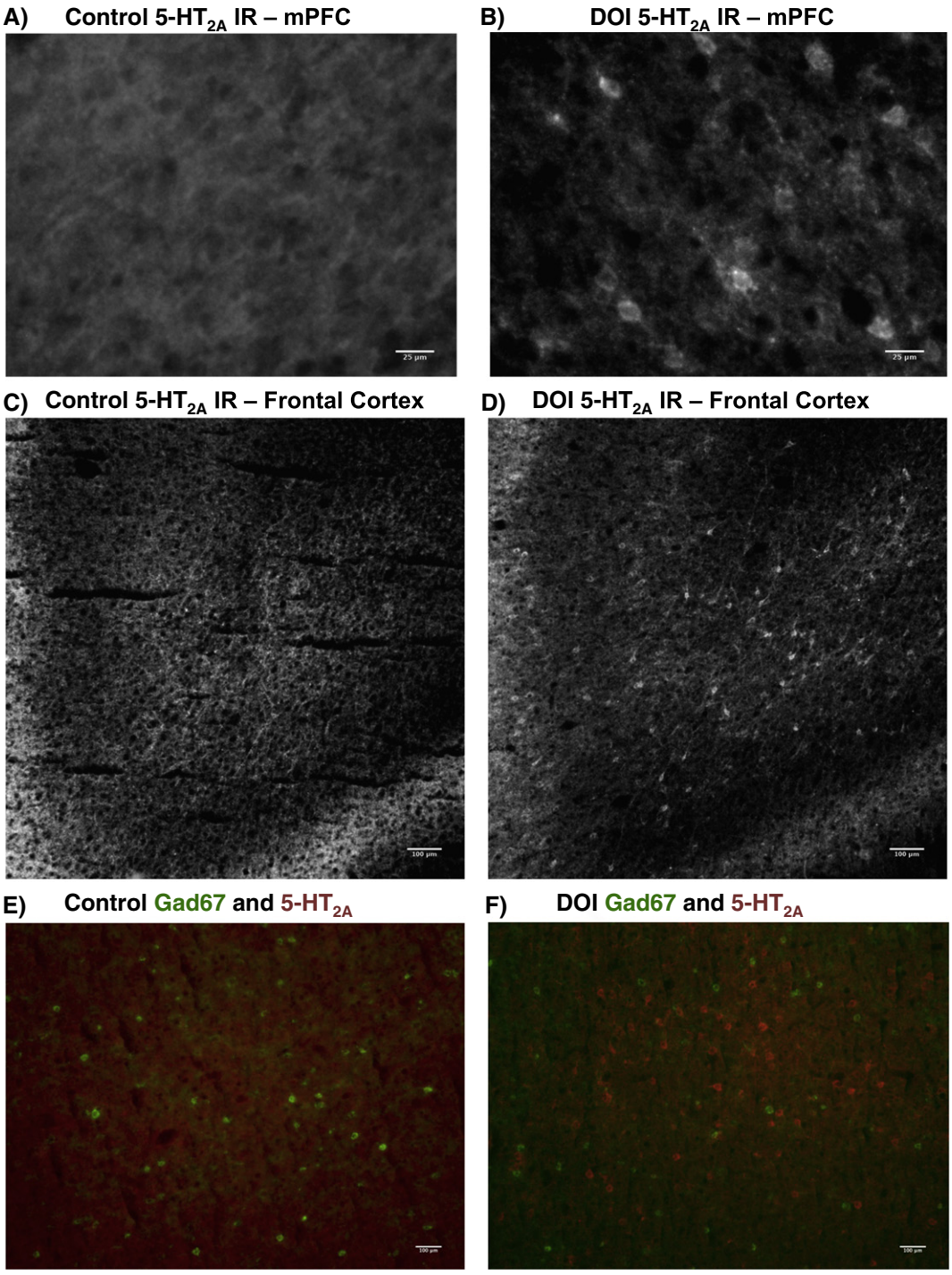

Fig. 6. (*R*)-DOI induces 5-HT$_{2A}$ receptor internalization within 5-HT$_{2A}$(+) cells: A,B) 40× view of 5-HT$_{2A}$-IR of deep layer V in prelimbic cortex of control (A) and treated (B) sections. C,D) 10× view of 5-HT$_{2A}$-IR in the lateral orbital cortex and agranular insular cortex (+4.2 mm from bregma) is shown in control (C) and treated (D) sections. E,F) 10× view of orbital cortex showing overlay of 5-HT$_{2A}$-IR (red) and Gad67-IR (green) in control (E) and treated (F) sections.

areas contained abundant, clearly labeled 5-HT$_{2A}$-IR cells that both did and did not produce cFos in response to (*R*)-DOI (Fig. 7). Superficial 5-HT$_{2A}$(+) neurons in the motor cortex (Fig. 7D–G) and the SSC were also co-labeled with cFos. Interestingly, although many cells bind (*R*)-DOI and respond by internalizing 5-HT$_{2A}$ receptors, only a fraction of these cells respond by producing cFos. Further, many cells that do not exhibit apparent 5-HT$_{2A}$ IR do express cFos in response to (*R*)-DOI (i.e., Fig. 7).

3.8. New FACS Methodology Permits Cell-Type Specific Sorting

Our initial FACS experiments demonstrate that subsets of a variety of cell types are transcriptionally activated by (*R*)-DOI, including 5-HT$_{2A}$, somatostatin, and parvalbumin expressing neurons. However, most neurons of these classes remain transcriptionally quiescent upon psychedelic administration. Isolation of specific neuronal populations would permit queries concerning molecular differences between

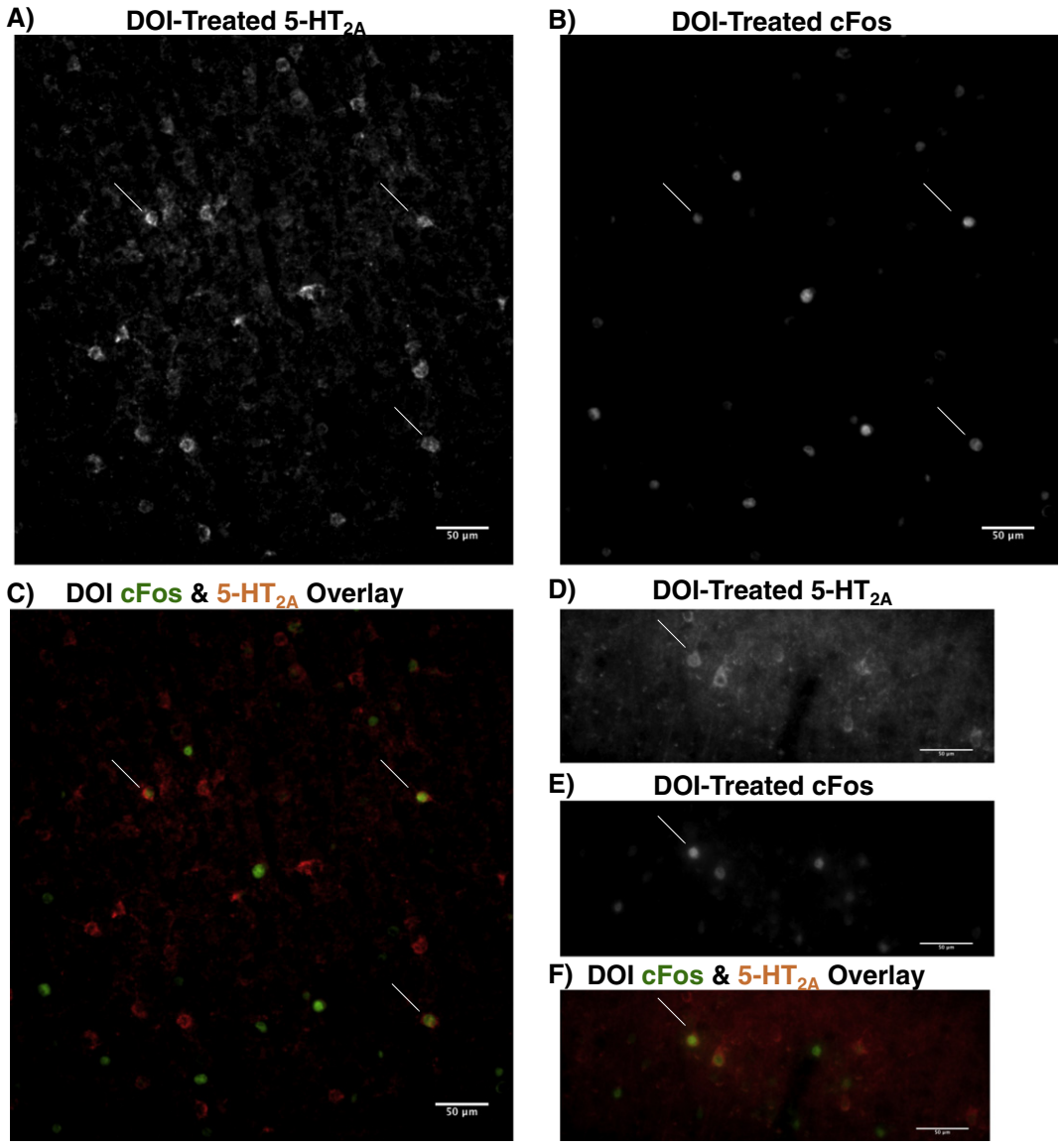

Fig. 7. (*R*)-DOI induces cFos in some 5-HT$_{2A}$(+) neurons: A,B,C) 20× view of deep PFC (+4.2 mm from bregma) from treated rat, showing 5-HT$_{2A}$-IR (A), cFos-IR (B), and the overlay of both stains (C). Arrows mark double-labeled cells. D,E,F) 20× view of superficial motor cortex (+2.7 mm from bregma) from treated rat, showing 5-HT$_{2A}$-IR (D), cFos-IR (E), and the overlay of both stains (F). Arrows mark double-labeled cells.

activated and non-activated neurons from a specified cell type. Previously described FACS methods (Guez-Barber et al., 2012), akin to our Method A, isolate neurons from initially unfixed brains. These methods result in small cell bodies composed primarily of a nucleus and depleted of all processes and most of the cytoplasm (see Fig. 1). In our hands, we found that staining for cytoplasmic and extracellular proteins including parvalbumin, somatostatin, Gad67, and 5-HT$_{2A}$ was not possible in these preparations. Therefore, we developed methodology to prepare neurons for FACS that fixes proteins prior to dissociation, but still allows for dissociation and downstream RNA analysis (*Experimental Procedures*, Method B). Microscopic analysis of these cells demonstrates that sorted neurons retain soluble cytosolic proteins, including parvalbumin and somatostatin (Fig. 10).

Initially, SOM cells were purified with FACS using Method B on SSC from fresh, immersion-fixed tissue obtained from treated and control animals (N = 4/group) (Fig. 8). Sorted SOM(+) neurons under control conditions exhibited very little cFos-IR, whereas a marked induction was apparent in a subset of SOM(+) neurons from animals treated with (*R*)-DOI (Fig. 8). We segregated 4 groups of neurons for sorting from the (*R*)-DOI group: DOI-SOM(+)/cFos(+); DOI-SOM(+)/cFos(−); DOI-SOM(−)/cFos(+); DOI-SOM(−)/cFos(−). We did not sort SOM(+)/cFos(+) neurons in controls as this population was exceedingly small. Therefore, three neuronal groups were sorted from the control group: CON-SOM(+); CON-SOM(−)/cFos(+); CON-SOM(−)/cFos(−) (Fig. 8). To determine the purity of neurons sorted with our FACS strategy, we measured the levels of *sst*, *slc17a7*, and *cfos* in each of the 7 sorted populations (Fig. 11; Table 1). QPCR analysis verified that all SOM(+) populations were highly enriched in *sst* and depleted in *slc17a7* when compared to SOM(−) populations, in both control and (*R*)-DOI groups (Fig. 11; Table 1). We also found that DOI-SOM(+)/cFos(+) neurons contained high levels of *cfos* mRNA equal to DOI-SOM(−)/cFos(+) neurons, and significantly more than all other populations (Fig. 8, Table S1). Conversely, DOI-SOM(+)/cFos(−) neurons have low levels of *cfos* similar to Control-SOM(+) neurons (Fig. 11). These results indicate that (*R*)-DOI highly transcriptionally activates a subset of SOM(+) neurons, whereas the majority remain quiescent. Comparison of SOM(+)/cFos(+) cells to SOM(+)/Fos(−) cells revealed that activated and non-activated somatostatin neurons

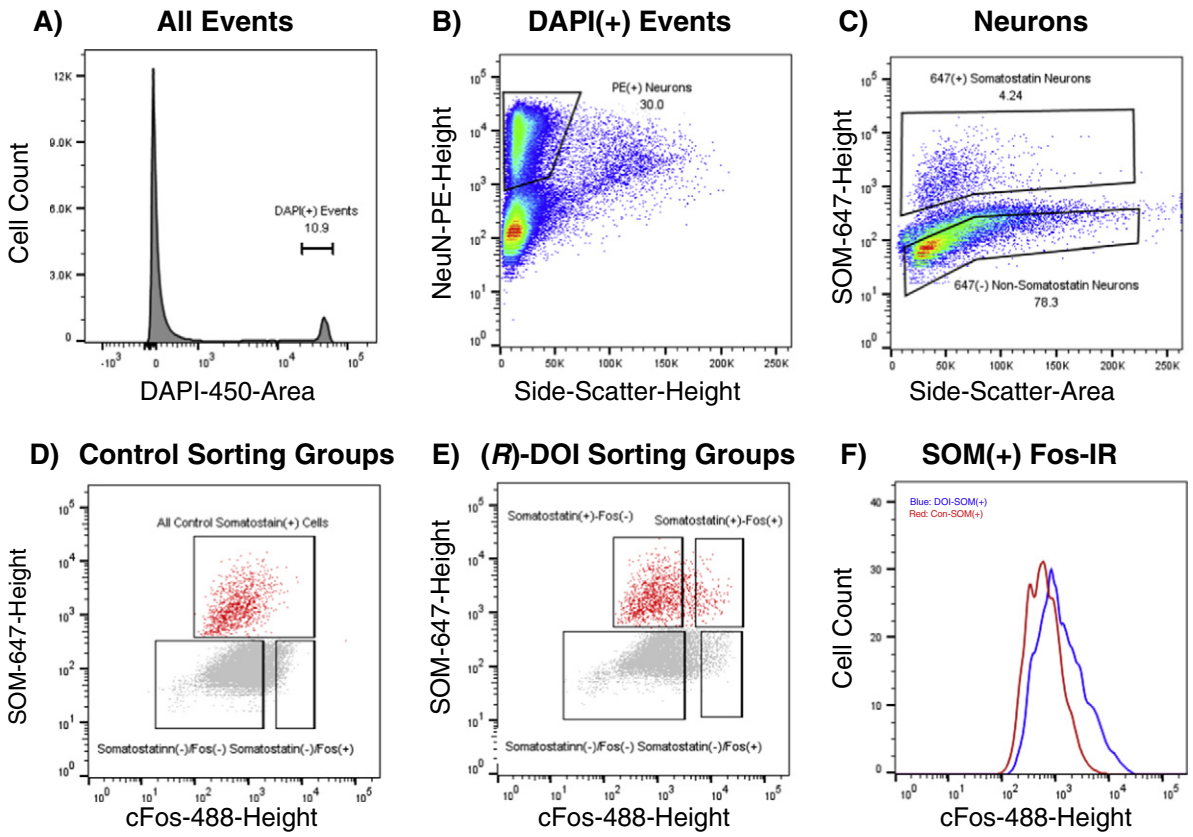

Fig. 8. FACS gating for SSC Somatostatin neurons: Data are from a representative sort; all runs produced similar patterns. Numbers represent percentages of cells within gates. A) All events are shown. DAPI(+) gate includes cells and excludes debris. B) NeuN-PE-Height/SideScatter-Height gate eliminates non-neurons and irregularly-shaped DAPI(+) events. C) Neurons are gated on Somatostatin-647-Height to select SOM(+) and SOM(−) neurons. D) 3 Control groups are gated: SOM(+), SOM(−)/Fos(+), and SOM(−)/Fos(−). E) 4 treated groups are gated: SOM(+)/Fos(+), SOM(+)/Fos(−), SOM(−)/Fos(+), SOM(−)/Fos(−). F) Histogram of cFos-immunoreactivity for all SOM(+) neurons from (*R*)-DOI (red) and control (blue) tissues.

express similar, low levels of *htr2a* mRNA (Fig. S6, Table 1). We interpret this to mean that SOM(+) neurons are primarily indirectly activated by (*R*)-DOI.

We also examined parvalbumin expressing neurons, which have been reported to express EGFP in *htr2a*-EGFP mice (Weber and Andrade, 2010). The gating strategy for sorting parvalbumin(+) (PV(+)) neurons is analogous to that used for sorting SOM(+) neurons, (Fig. 9). As expected from our earlier FACS studies, PV(+) neurons in the mPFC contain little cFos-IR under control conditions, whereas a significant fraction become highly activated in response to (*R*)-DOI (Fig. 9). We verified that sorted populations were pure, as all groups of PV(+) neurons displayed high levels of *pvlb* and low levels of *slc17a7* relative to PV(−) neurons (Fig. 11; Table 1). We also confirmed that DOI-PV(+)/cFos(+) neurons contained very high levels of *cfos* mRNA, equivalent to DOI-PV(−)/− cFos(+) neurons, and higher than every other group (Fig. 11). Conversely, DOI-PV(+)/cFos(−) neurons have low levels of *fos*, similar to CON-PV(+) neurons (Fig. 11). These results support our FACS analysis (Fig. 9F), which shows that a subset of PV(+) neurons become activated by (*R*)-DOI, while the majority remain quiescent. Comparing activated PV(+) neurons to non-activated neurons within the (*R*)-DOI group, we did not observe a statistically significant increase in *htr2a* expression (Fig. S6), although PV(+) neurons express *htr2a* at a level similar to or higher than that seen in PV(−) populations (Fig. S7, Table 1). These results suggest that direct binding to and activation of PV(+) neurons by (*R*)-DOI may not be a critical factor in their activation, consistent with a primarily indirect mechanism of activation of PV(+) neurons by psychedelics.

Table 1
Summary of cell-type specific marker gene expression: All samples of sorted cells from a particular neuronal subtype PV(+), PV(−), SOM(+), and SOM(−), were grouped together and gene expression levels are shown for select genes. Numbers represent percentage changes (±SEM) relative to PV(−) (top 2 rows) or SOM(−) (bottom 2 rows), using *gapdh* to normalize. PV(+), SOM(+), N = 12; PV(−), SOM(−), N = 16. Students t-test, "***" indicates $p < 0.001$.

	Sst	*Slc17a7*	*Htr2a*
All SOM(+)	4382 ± 590%***	6.09 ± 1.72%***	26.7 ± 8.6%***
All SOM(−)	100 ± 18.3%	100 ± 7.9%	100 ± 10.6%
	Pvlb	*Slc17a7*	*Htr2a*
All PV(+)	3401 ± 801%***	6.04 ± 1.27%***	140 ± 29.0% (ns)
All PV(−)	100 ± 43.7%	100 ± 10.22%	100 ± 12.4%

3.9. IEG Induction Varies across Cell Types

Although levels of *cfos* induction among SOM(+) and PV(+) neurons that were cFos(+) were similar to levels of *cfos* induction in activated SOM(−) and PV(−) neurons following (*R*)-DOI, we asked whether other IEGs might exhibit cell-type specific activation patterns. Interestingly, we found that all groups of sorted SOM(+) interneurons display similar levels of *egr2*, regardless of their activation state, whereas PV(+) interneurons never contained *egr2*, regardless of activation state (Fig. 11). Within PV(−) and SOM(−) populations, the expected pattern of *egr2* induction was measured between activated and non-activated neurons, based on our initial FACS and QPCR studies (Fig. 11). These results demonstrate that heterogeneous transcriptional responses occur between different neuronal types following psychedelic administration, despite similar induction of cFos protein and *fos* mRNA.

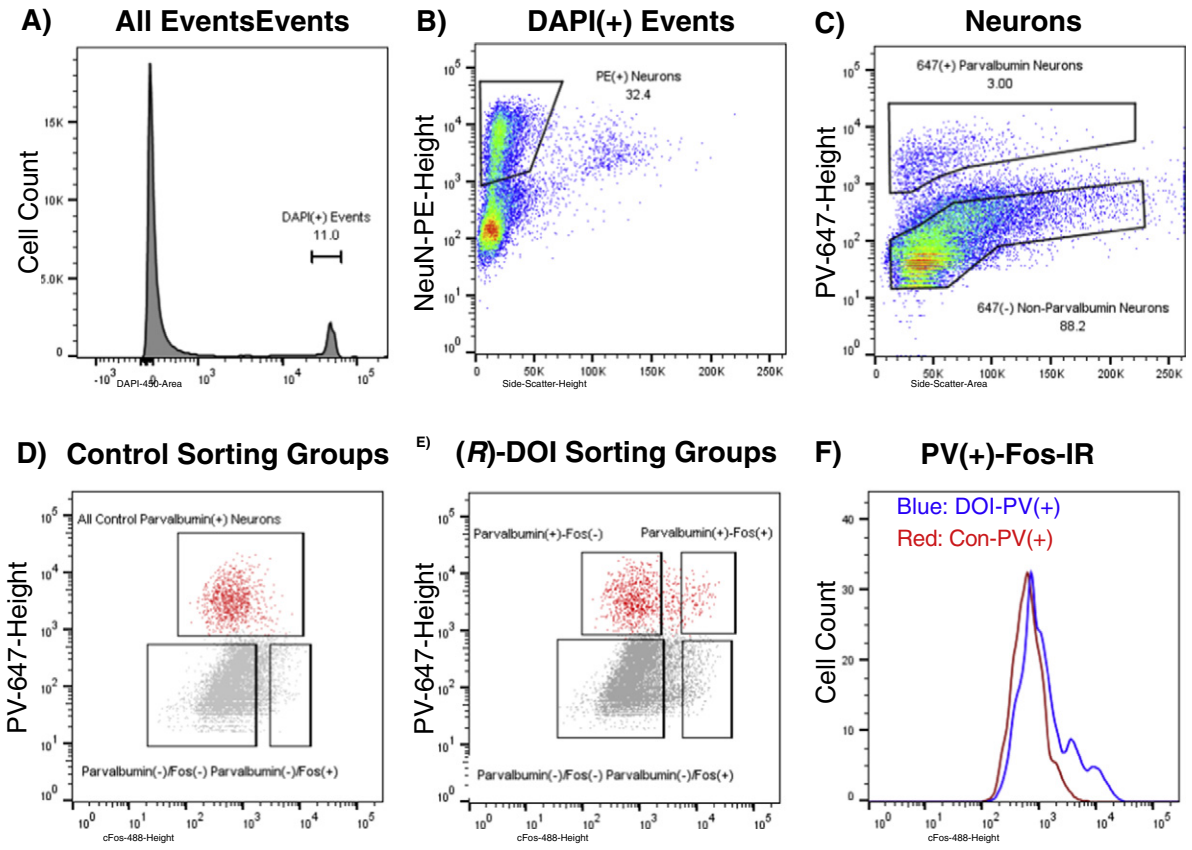

Fig. 9. FACS gating for mPFC Parvalbumin neurons: Data are from a representative sort; all runs produced similar patterns. Numbers represent percentages of cells within gates. A) All events are shown. DAPI(+) gate includes cells and excludes debris. B) NeuN-PE-Height/SideScatter-Height gate eliminates non-neurons and irregularly-shaped DAPI(+) events. C) Neurons are gated on Parvalbumin-647-Height to select PV(+) and PV(−) neurons. D) 3 Control groups are gated: PV(+), PV(−)/Fos(+), and PV(−)/Fos(−). E) 4 treated groups are gated: PV(+)/Fos(+), PV(+)/Fos(−), PV(−)/Fos(+), PV(−)/Fos(−). F) Histogram of cFos-immunoreactivity for all PV(+) neurons from (*R*)-DOI (red) and control (blue) tissues.

4. Discussion

Our results indicate that (*R*)-DOI transcriptionally activates heterogeneous populations of inhibitory and excitatory cells in both mPFC and SSC. The activated excitatory neuronal cell populations express higher levels of 5-HT_{2A} receptor mRNA in mPFC, and higher levels of both 5-HT_{2A} and mGluR2 receptor mRNA in SSC. Neurons containing the highest levels of phosphorylated (Ser32) cFos express levels of *htr2a* approximately 3–4 times that of (Ser32) cFos positive neurons of the control treatment group. We confirmed with immunofluorescence microscopy that a small subset of 5-HT_{2A} receptor-expressing neurons produces cFos in response to (*R*)-DOI in the mPFC, SSC, orbital cortex, and claustrum. Although this result might be anticipated because 5-HT_{2A} receptor activation is necessary for psychedelic-induced responses, several previous studies have each failed to co-localize cFos to 5-HT_{2A}-IR cells (Mackowiak et al., 1999; Pei et al., 2004; Scruggs et al., 2000). One potential explanation is that these studies used a 5-HT_{2A} receptor monoclonal antibody from Pharmingen that is no longer available. By contrast, one study has shown cFos induction within 5-HT_{2A} cells of the SSC following DOI, using a different antibody (ab16028, Abcam, discontinued)(Hazama et al., 2014). Neither of these two receptor antibodies, however, has been extensively verified for specificity in *htr2a* knockout animals, whereas the antibody we employed in our studies has been validated (Magalhaes et al., 2010; Weber and Andrade, 2010).

We hypothesize that the small population of excitatory neurons expressing increased levels of *htr2A* mRNA that are directly activated by (*R*)-DOI represent a "trigger population", and are neurons that depolarize upon exposure to psychedelics. Further, we propose that activation of these neurons initiates the events leading to recurrent activity, cortical network destabilization, and the host of perceptual and cognitive behaviors associated with psychedelics. Our results indicate that a large number of 5-HT_{2A}-expressing cells undergo dramatic receptor redistribution to the soma following (*R*)-DOI in all frontal areas that normally express 5-HT_{2A} receptors, and we have also observed this phenomena following LSD (unpublished observations). These results are consistent with agonist-induced receptor internalization, which has been observed previously for the 5-HT_{2A} receptor in vitro (Berry et al., 1996; Karaki et al., 2014). Interestingly, many neurons that internalize 5-HT_{2A} receptors upon (*R*)-DOI administration do not express cFos. Furthermore, most neurons that produce cFos in response to (*R*)-DOI do not express appreciable levels of 5-HT_{2A} receptors. Future studies are necessary to determine the differences between 5-HT_{2A}-expressing cells that do and do not become activated by psychedelics.

The data we present here are from animals treated with a singular, high dose of (*R*)-DOI. We chose a dose that was likely to produce near maximum increases in cFos induction (Leslie et al., 1993) in order to produce robust signals for our FACS separations and downstream mRNA analyses. However, we note that despite the high dose given, IEG induction is still primarily restricted to a relatively small group of highly activated neurons. Also, while (*R*)-DOI does have affinity for the 5-HT_{2C} receptors, which modifies its effects on behavior, we did not find that *htr2c* levels were differentially distributed between treated animals and controls with respect to activated and non-activated neurons, in contrast to enriched *htr2a* levels in (*R*)-DOI activated cells. Furthermore, we have observed in preliminary experiments a similar induction of cFos in 5-HT_{2A}-expressing cells following LSD (0.5 mg/kg, i.p.). Nevertheless, it will be important to observe the cellular effects

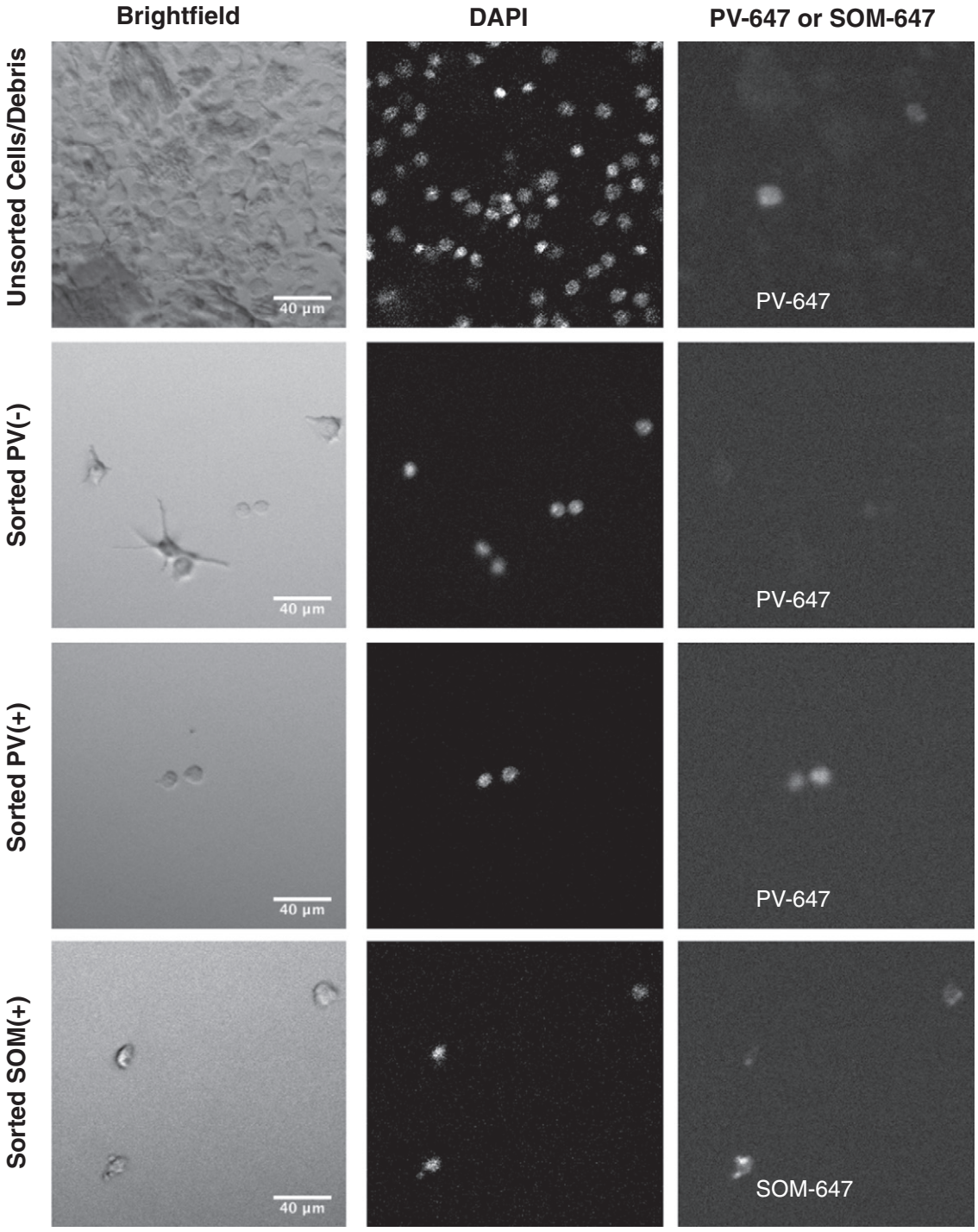

Fig. 10. Images of sorted interneurons: Panel shows representative images of cells sorted using Method B, viewed at 60×. Filters used include brightfield (left), DAPI (center), and 647 (right). Cells include unsorted, dissociated tissue, including cells and debris (top row), sorted PV(−) neurons (2nd row), sorted PV(+) neurons (3rd row), and sorted SOM(+) neurons (4th row). Note that sorted cells contain occasional PV(+) neurons and sorted cells retain cytoplasmic proteins.

of a wider variety of psychedelics, which posses varying receptor-binding profiles, at a variety of doses to generalize the responses observed here.

The primary inhibitory interneuron populations activated by (*R*)-DOI are the somatostatin and parvalbumin neurons. For both types of interneurons, only a small subset of the total number of interneurons

Fig. 11. QPCR analysis of sorted interneurons: A) High levels of *sst* are found in SOM(+) cells, but not SOM(−) cells. B) High levels of *pvlb* are found in PV(+) cells but not PV(−) cells. C) Low levels of *slc17a7* are found in SOM(+) cells relative to SOM(−) cells. D) Low levels of *slc17a7* are found in PV(+) cells relative to PV(−) cells. E) DOI-SOM(+)/Fos(+) cells have high levels of *fos*. F) DOI-PV(+)/Fos(+) cells have high levels of *fos*. G) DOI-SOM(+)/Fos(+) cells have levels of *egr2* similar to DOI-SOM(+)/Fos(−) cells. H) *Egr2* is not expressed in PV(+) cells. In each panel, one-way ANOVA & Tukey post-hoc test was performed between all groups (N = 4/group) and full statistics can be found in Tables S1, S2. Only select comparisons are illustrated here for clarity. Symbols "*", "**", and "****" indicate $p < 0.05$, $p < 0.01$, and $p < 0.001$, respectively.

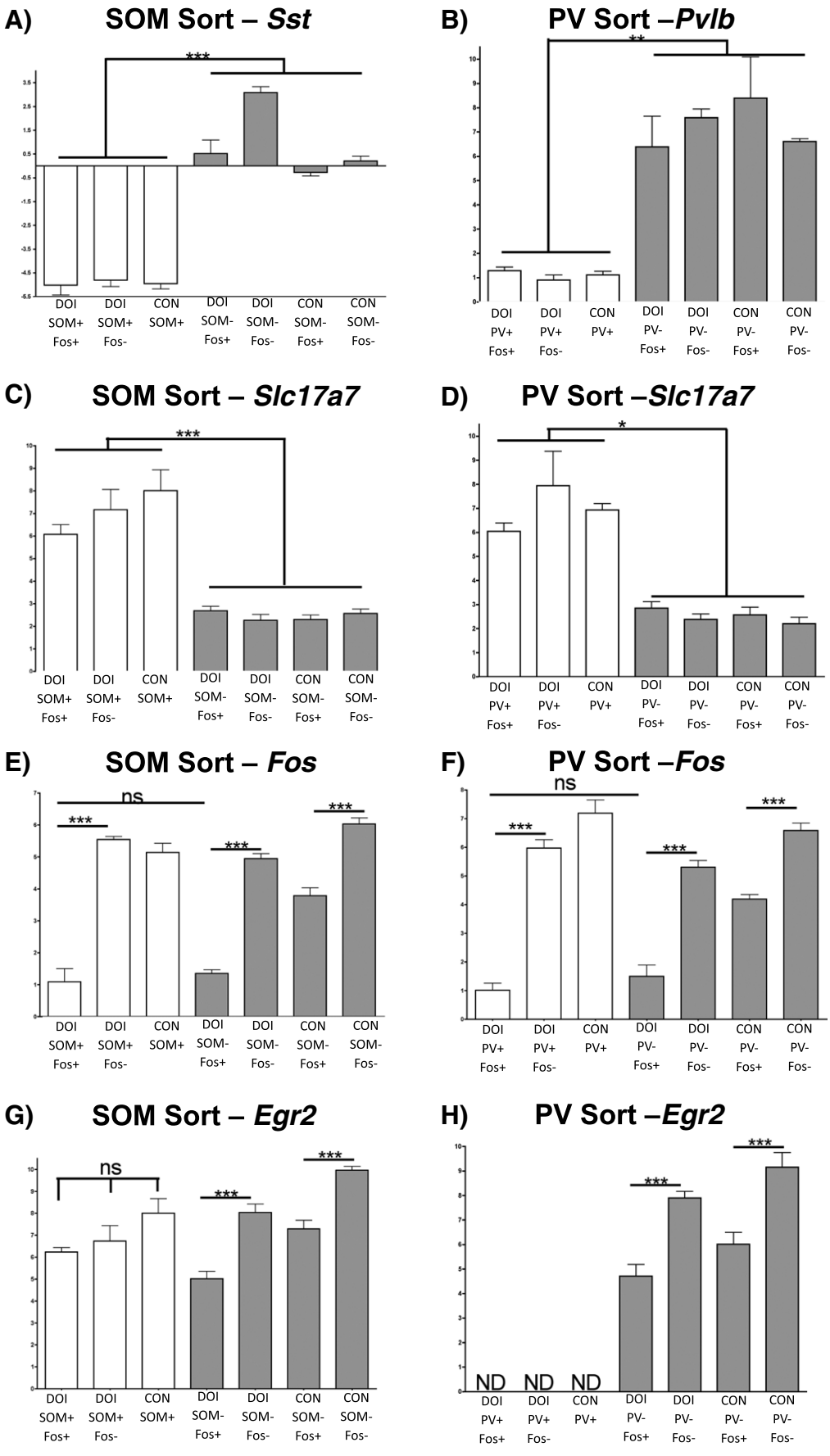
A)
SOM Sort – Sst
***
DOI SOM+ Fos+
DOI SOM+ Fos-
CON SOM+
DOI SOM- Fos+
DOI SOM- Fos-
CON SOM- Fos+
CON SOM- Fos-
B)
PV Sort –Pvlb
**
DOI PV+ Fos+
DOI PV+ Fos-
CON PV+
DOI PV- Fos+
DOI PV- Fos-
CON PV- Fos+
CON PV- Fos-
C)
SOM Sort – Slc17a7
***
D)
PV Sort –Slc17a7
*
E)
SOM Sort – Fos
ns
***
F)
PV Sort –Fos
ns
***
G)
SOM Sort – Egr2
ns
***
H)
PV Sort –Egr2
ND
***

are activated. One hypothesis is that interneurons, a subset of which express 5-HT_{2A} receptors, are directly bound and activated by psychedelics, as demonstrated in slices (Weber and Andrade, 2010; Zhou and Hablitz, 1999). In our studies we did not find a substantial enrichment of *htr2a* in activated interneurons relative to non-activated interneurons. Also, co-staining between Gad67-IR and 5-HT_{2A}-IR showed that the majority of clearly labeled 5-HT_{2A}(+) cells in the drug-treated condition were excitatory, although deep layers of the parietal cortex occasionally contained double-labeled cells, and PV(+) cells do express *htr2a*. While these data do not preclude the possibility that some interneurons are modulated by direct actions of (*R*)-DOI, they indicate that interneuron activation by psychedelics is probably indirect, and in response to increases in cortical neural activity. Interestingly, activated somatostatin interneurons do not produce *egr2* in response to (*R*)-DOI, and parvalbumin interneurons do not produce *egr2* in either baseline or activated states. *Egr2* induction in the cortex has been proposed to be a marker for psychedelic activation of 5-HT_{2A} receptors (Gonzalez-Maeso et al., 2003). Our results indicate that *egr2* induction is restricted to particular cell types in response to psychedelics, and is not a generally induced marker. Further studies will be required to examine more fully the nature of cell-type specific IEG induction and the importance of these effects for effecting long-term cellular changes.

The functional consequences of interneuron activation with respect to psychedelic-induced behaviors are likely important, and this area remains unexplored. Psychedelics markedly affect the local field potential (LFP) in the gamma frequency range (Wood et al., 2012), which is largely modulated by GABAergic cells. Neuronal oscillations are important in coordinating information transfer throughout the brain and disruption of these rhythms might be a critical component of the diverse effects of psychedelics (Muthukumaraswamy et al., 2013). In our previous studies of long-term LSD administration, we found a variety of GABA-related mRNA expression abnormalities weeks after drug administration was halted, implicating persistent dysregulation (Martin et al., 2014). Additionally, the consistent finding of GABA-related molecular changes in the cortex of psychiatric patients (Gonzalez-Burgos and Lewis, 2008) warrants additional investigations into the function of these cells in normal and abnormal states.

In addition to neuronal activation, subpopulations of non-neurons, including astrocytes, respond to (*R*)-DOI by producing *fos* and *per1*. *Per1* is a core component of the circadian clock and its expression has been shown to cycle in astrocytes (Prolo et al., 2005). Although global brain *per1* mRNA levels are known to increase in response to psychedelics (Gonzalez-Maeso et al., 2003), regulation of its, or any other gene's, transcription by psychedelics in astrocytes has not been previously examined. The meaning and functional consequences of this response are unknown, but the idea that astrocytes may be involved with electrophysiological responses to psychedelics has been proposed (Aghajanian, 2009). Astrocytes are also known to be extensively involved in regulating metabolic substrate transport to neurons (Gandhi et al., 2009), as well as blood flow to local areas of the brain (Zonta et al., 2003). Psychedelics are known to increase glucose utilization in the cortex (Vollenweider et al., 1997), and cerebral glucose is primarily removed from the blood by astrocytes. Interestingly, blood flow and BOLD responses in the cortex are decreased following psilocybin (Carhart-Harris et al., 2012), leaving open questions surrounding neurovascular coupling during the psychedelic state (Spain et al., 2015). Activation of particular cell types, including astrocytes and interneurons, may play separable roles in neurovascular responses.

In order to study neuronal subtype-specific drug effects, we developed FACS methods applicable for robust sorting of cortical cells based on soluble cytosolic proteins that preserve RNA. Using this methodology we segregated and separately analyzed populations of both parvalbumin and somatostatin interneurons for this study. We have also validated this methodology to sort based upon extracellular membrane proteins and in routinely fixed human post-mortem brain (unpublished data). Populations of cells are likely >94% pure, as *slc17a7* is reduced by this amount in both SOM(+) and PV(+) cells (Table 1). Sort purity may be higher, because some *slc17a7* expression is expected in these cell types, as *slc17a7* has been detected in interneurons by single cell QPCR (Rossier et al., 2015). It should be noted that while mRNA moieties present in the cytoplasm are preserved with this protocol, genetic information located in the processes, such as dendrites and axons, is not preserved as most processes are lost during the FACS procedures.

Significantly, the ability to quickly separate large populations of brain cells based on a wide variety of soluble, cytosolic, and extracellular membrane proteins and retain mRNA stability will expand the utility of FACS in the neurosciences. Currently, to isolate highly enriched populations of cells based on cytosolic or extracellular membrane proteins relies on the laborious and low throughput method of laser capture microdissection. Neurocytometry can now be employed to isolate large and multiple populations of cells from a single block of brain tissue to study cell-type specific transcriptional responses to drug administration, environmental manipulation, and disease progression, and only requires access to flow cytometry infrastructure.

Funding Sources

This work was partially funded by NIH grants R01MH083689, P30GM106392, and the Heffter Research Institute.

Conflict of Interest

The authors declare no conflict of interest.

Author Contributions

D.A.M. designed, conducted, and interpreted data from experiments as well as write the manuscript. C.D.N designed experiments, interpreted data, and edited the manuscript.

Acknowledgements

We would like to thank Dr. Bruce Hope and Dr. Javier Rubio for training in neuronal dissociation, Dr. David Nichols for synthesis of (*R*)-DOI, Connie Porretta for expertise in flow cytometry, along with Patrick White and Maxwell Norleans for laboratory assistance.

Appendix A. Supplementary data

Supplementary data to this article can be found online at http://dx.doi.org/10.1016/j.ebiom.2016.08.049.

References

Abi-Saab, W.M., Bubser, M., Roth, R.H., Deutch, A.Y., 1999. 5-HT2 receptor regulation of extracellular GABA levels in the prefrontal cortex. Neuropsychopharmacology 20, 92–96.

Aghajanian, G.K., 2009. Modeling "psychosis" in vitro by inducing disordered neuronal network activity in cortical brain slices. Psychopharmacology 206, 575–585.

Beique, J.C., Imad, M., Mladenovic, L., Gingrich, J.A., Andrade, R., 2007. Mechanism of the 5-hydroxytryptamine 2A receptor-mediated facilitation of synaptic activity in prefrontal cortex. Proc. Natl. Acad. Sci. U. S. A. 104, 9870–9875.

Benneyworth, M.A., Xiang, Z., Smith, R.L., Garcia, E.E., Conn, P.J., Sanders-Bush, E., 2007. A selective positive allosteric modulator of metabotropic glutamate receptor subtype 2 blocks a hallucinogenic drug model of psychosis. Mol. Pharmacol. 72, 477–484.

Berry, S.A., Shah, M.C., Khan, N., Roth, B.L., 1996. Rapid agonist-induced internalization of the 5-hydroxytryptamine2A receptor occurs via the endosome pathway in vitro. Mol. Pharmacol. 50, 306–313.

Bogenschutz, M.P., Forcehimes, A.A., Pommy, J.A., Wilcox, C.E., Barbosa, P.C., Strassman, R.J., 2015. Psilocybin-assisted treatment for alcohol dependence: a proof-of-concept study. J. Psychopharmacol. 29, 289–299.

Carhart-Harris, R.L., Erritzoe, D., Williams, T., Stone, J.M., Reed, L.J., Colasanti, A., Tyacke, R.J., Leech, R., Malizia, A.L., Murphy, K., et al., 2012. Neural correlates of the psychedelic state as determined by fMRI studies with psilocybin. Proc. Natl. Acad. Sci. U. S. A. 109, 2138–2143.

Gandhi, G.K., Cruz, N.F., Ball, K.K., Dienel, G.A., 2009. Astrocytes are poised for lactate trafficking and release from activated brain and for supply of glucose to neurons. J. Neurochem. 111, 522–536.
Gasser, P., Kirchner, K., Passie, T., 2014. LSD-assisted psychotherapy for anxiety associated with a life-threatening disease: a qualitative study of acute and sustained subjective effects. J. Psychopharmacol.
Gewirtz, J.C., Marek, G.J., 2000. Behavioral evidence for interactions between a hallucinogenic drug and group II metabotropic glutamate receptors. Neuropsychopharmacology 23, 569–576.
Glennon, R.A., Titeler, M., McKenney, J.D., 1984. Evidence for 5-HT2 involvement in the mechanism of action of hallucinogenic agents. Life Sci. 35, 2505–2511.
Gonzalez-Burgos, G., Lewis, D.A., 2008. GABA neurons and the mechanisms of network oscillations: implications for understanding cortical dysfunction in schizophrenia. Schizophr. Bull. 34, 944–961.
Gonzalez-Maeso, J., Yuen, T., Ebersole, B.J., Wurmbach, E., Lira, A., Zhou, M., Weisstaub, N., Hen, R., Gingrich, J.A., Sealfon, S.C., 2003. Transcriptome fingerprints distinguish hallucinogenic and nonhallucinogenic 5-hydroxytryptamine 2A receptor agonist effects in mouse somatosensory cortex. J. Neurosci. 23, 8836–8843.
Gonzalez-Maeso, J., Weisstaub, N.V., Zhou, M., Chan, P., Ivic, L., Ang, R., Lira, A., Bradley-Moore, M., Ge, Y., Zhou, Q., et al., 2007. Hallucinogens recruit specific cortical 5-HT(2A) receptor-mediated signaling pathways to affect behavior. Neuron 53, 439–452.
Gresch, P.J., Barrett, R.J., Sanders-Bush, E., Smith, R.L., 2007. 5-Hydroxytryptamine (serotonin)2A receptors in rat anterior cingulate cortex mediate the discriminative stimulus properties of d-lysergic acid diethylamide. J. Pharmacol. Exp. Ther. 320, 662–669.
Grob, C.S., Danforth, A.L., Chopra, G.S., Hagerty, M., McKay, C.R., Halberstadt, A.L., Greer, G.R., 2011. Pilot study of psilocybin treatment for anxiety in patients with advanced-stage cancer. Arch. Gen. Psychiatry 68, 71–78.
Guez-Barber, D., Fanous, S., Harvey, B.K., Zhang, Y., Lehrmann, E., Becker, K.G., Picciotto, M.R., Hope, B.T., 2012. FACS purification of immunolabeled cell types from adult rat brain. J. Neurosci. Methods 203, 10–18.
Halberstadt, A.L., 2015. Recent advances in the neuropsychopharmacology of serotonergic hallucinogens. Behav. Brain Res. 277, 99–120.
Halberstadt, A.L., Geyer, M.A., 2011. Multiple receptors contribute to the behavioral effects of indoleamine hallucinogens. Neuropharmacology 61, 364–381.
Hazama, K., Hayata-Takano, A., Uetsuki, K., Kasai, A., Encho, N., Shintani, N., Nagayasu, K., Hashimoto, R., Reglodi, D., Miyakawa, T., et al., 2014. Increased behavioral and neuronal responses to a hallucinogenic drug in PACAP heterozygous mutant mice. PLoS One 9, e89153.
Johnson, M.W., Garcia-Romeu, A., Cosimano, M.P., Griffiths, R.R., 2014. Pilot study of the 5-HT2AR agonist psilocybin in the treatment of tobacco addiction. J. Psychopharmacol. 28, 983–992.
Karaki, S., Becamel, C., Murat, S., Mannoury la Cour, C., Millan, M.J., Prezeau, L., Bockaert, J., Marin, P., Vandermoere, F., 2014. Quantitative phosphoproteomics unravels biased phosphorylation of serotonin 2A receptor at Ser280 by hallucinogenic versus nonhallucinogenic agonists. Mol. Cell. Proteomics 13, 1273–1285.
Kubota, Y., Kawaguchi, Y., 1994. Three classes of GABAergic interneurons in neocortex and neostriatum. Jpn. J. Physiol. 44 (Suppl 2), S145–S148.
Leslie, R.A., Moorman, J.M., Coulson, A., Grahame-Smith, D.G., 1993. Serotonin2/1C receptor activation causes a localized expression of the immediate-early gene c-fos in rat brain: evidence for involvement of dorsal raphe nucleus projection fibres. Neuroscience 53, 457–463.
Liu, Q.R., Rubio, F.J., Bossert, J.M., Marchant, N.J., Fanous, S., Hou, X., Shaham, Y., Hope, B.T., 2014. Detection of molecular alterations in methamphetamine-activated Fos-expressing neurons from a single rat dorsal striatum using fluorescence-activatedcell sorting (FACS). J. Neurochem. 128, 173–185.
Mackowiak, M., Chocyk, A., Fijal, K., Czyrak, A., Wedzony, K., 1999. c-Fos proteins, induced by the serotonin receptor agonist DOI, are not expressed in 5-HT2A positive cortical neurons. Brain Res. Mol. Brain Res. 71, 358–363.
Magalhaes, A.C., Holmes, K.D., Dale, L.B., Comps-Agrar, L., Lee, D., Yadav, P.N., Drysdale, L., Poulter, M.O., Roth, B.L., Pin, J.P., et al., 2010. CRF receptor 1 regulates anxiety behavior via sensitization of 5-HT2 receptor signaling. Nat. Neurosci. 13, 622–629.
Marek, G.J., Wright, R.A., Schoepp, D.D., Monn, J.A., Aghajanian, G.K., 2000. Physiological antagonism between 5-hydroxytryptamine(2A) and group II metabotropic glutamate receptors in prefrontal cortex. J. Pharmacol. Exp. Ther. 292, 76–87.
Martin, D.A., Marona-Lewicka, D., Nichols, D.E., Nichols, C.D., 2014. Chronic LSD alters gene expression profiles in the mPFC relevant to schizophrenia. Neuropharmacology 83, 1–8.
Muthukumaraswamy, S.D., Carhart-Harris, R.L., Moran, R.J., Brookes, M.J., Williams, T.M., Errtizoe, D., Sessa, B., Papadopoulos, A., Bolstridge, M., Singh, K.D., et al., 2013. Broadband cortical desynchronization underlies the human psychedelic state. J. Neurosci. 33, 15171–15183.
Nichols, D.E., 2016. Psychedelics. Pharmacol. Rev. 68, 264–355.
Nichols, C.D., Sanders-Bush, E., 2002. A single dose of lysergic acid diethylamide influences gene expression patterns within the mammalian brain. Neuropsychopharmacology 26, 634–642.
Nichols, C.D., Garcia, E.E., Sanders-Bush, E., 2003. Dynamic changes in prefrontal cortex gene expression following lysergic acid diethylamide administration. Brain Res. Mol. Brain Res. 111, 182–188.
Pasqualetti, M., Nardi, I., Ladinsky, H., Marazziti, D., Cassano, G.B., 1996. Comparative anatomical distribution of serotonin 1A, 1D alpha and 2A receptor mRNAs in human brain postmortem. Brain Res. Mol. Brain Res. 39, 223–233.
Pazos, A., Cortes, R., Palacios, J.M., 1985. Quantitative autoradiographic mapping of serotonin receptors in the rat brain. II. Serotonin-2 receptors. Brain Res. 346, 231–249.
Pei, Q., Tordera, R., Sprakes, M., Sharp, T., 2004. Glutamate receptor activation is involved in 5-HT2 agonist-induced Arc gene expression in the rat cortex. Neuropharmacology 46, 331–339.
Prolo, L.M., Takahashi, J.S., Herzog, E.D., 2005. Circadian rhythm generation and entrainment in astrocytes. J. Neurosci. 25, 404–408.
Reissig, C.J., Rabin, R.A., Winter, J.C., Dlugos, C.A., 2008. d-LSD-induced c-Fos expression occurs in a population of oligodendrocytes in rat prefrontal cortex. Eur. J. Pharmacol. 583, 40–47.
Riba, J., Anderer, P., Jane, F., Saletu, B., Barbanoj, M.J., 2004. Effects of the South American psychoactive beverage ayahuasca on regional brain electrical activity in humans: a functional neuroimaging study using low-resolution electromagnetic tomography. Neuropsychobiology 50, 89–101.
Rossier, J., Bernard, A., Cabungcal, J.H., Perrenoud, Q., Savoye, A., Gallopin, T., Hawrylycz, M., Cuenod, M., Do, K., Urban, A., et al., 2015. Cortical fast-spiking parvalbumin interneurons enwrapped in the perineuronal net express the metallopeptidases Adamts8, Adamts15 and Neprilysin. Mol. Psychiatry 20, 154–161.
Rudy, B., Fishell, G., Lee, S., Hjerling-Leffler, J., 2011. Three groups of interneurons account for nearly 100% of neocortical GABAergic neurons. Dev. Neuropsychol. 71, 45–61.
Sasaki, T., Kojima, H., Kishimoto, R., Ikeda, A., Kunimoto, H., Nakajima, K., 2006. Spatiotemporal regulation of c-Fos by ERK5 and the E3 ubiquitin ligase UBR1, and its biological role. Mol. Cell 24, 63–75.
Scruggs, J.L., Patel, S., Bubser, M., Deutch, A.Y., 2000. DOI-Induced activation of the cortex: dependence on 5-HT2A heteroceptors on thalamocortical glutamatergic neurons. J. Neurosci. 20, 8846–8852.
Spain, A., Howarth, C., Khrapitchev, A.A., Sharp, T., Sibson, N.R., Martin, C., 2015. Neurovascular and neuroimaging effects of the hallucinogenic serotonin receptor agonist psilocin in the rat brain. Neuropharmacology 99, 210–220.
Tilakaratne, N., Friedman, E., 1996. Genomic responses to 5-HT1A or 5-HT2A/2C receptor activation is differentially regulated in four regions of rat brain. Eur. J. Pharmacol. 307, 211–217.
Vollenweider, F.X., Leenders, K.L., Scharfetter, C., Maguire, P., Stadelmann, O., Angst, J., 1997. Positron emission tomography and fluorodeoxyglucose studies of metabolic hyperfrontality and psychopathology in the psilocybin model of psychosis. Neuropsychopharmacology 16, 357–372.
Vollenweider, F.X., Vollenweider-Scherpenhuyzen, M.F., Babler, A., Vogel, H., Hell, D., 1998. Psilocybin induces schizophrenia-like psychosis in humans via a serotonin-2 agonist action. Neuroreport 9, 3897–3902.
Weber, E.T., Andrade, R., 2010. Htr2a gene and 5-HT(2A) receptor expression in the cerebral cortex studied using genetically modified mice. Front. Neurosci. 4.
Wischhof, L., Koch, M., 2012. Pre-treatment with the mGlu2/3 receptor agonist LY379268 attenuates DOI-induced impulsive responding and regional c-Fos protein expression. Psychopharmacology 219, 387–400.
Wood, J., Kim, Y., Moghaddam, B., 2012. Disruption of prefrontal cortex large scale neuronal activity by different classes of psychotomimetic drugs. J. Neurosci. 32, 3022–3031.
Zhou, F.M., Hablitz, J.J., 1999. Activation of serotonin receptors modulates synaptic transmission in rat cerebral cortex. J. Neurophysiol. 82, 2989–2999.
Zonta, M., Angulo, M.C., Gobbo, S., Rosengarten, B., Hossmann, K.A., Pozzan, T., Carmignoto, G., 2003. Neuron-to-astrocyte signaling is central to the dynamic control of brain microcirculation. Nat. Neurosci. 6, 43–50.